Distance statistics in quadrangulations with no multiple edges and the geometry of minbus

2010 J. Phys. A: Math. Theor. 43 205207

(http://iopscience.iop.org/1751-8121/43/20/205207)

IOP PUBLISHING JOURNAL OF PHYSICS A: MATHEMATICAL AND THEORETICAL

J. Phys. A: Math. Theor. **43** (2010) 205207 (31pp) doi:10.1088/1751-8113/43/20/205207

Distance statistics in quadrangulations with no multiple edges and the geometry of minbus

J Bouttier and E Guitter

Institut de Physique Théorique, CEA, IPhT, F-91191 Gif-sur-Yvette, CNRS, URA 2306, France

E-mail: jeremie.bouttier@cea.fr and emmanuel.guitter@cea.fr

Received 16 February 2010, in final form 25 March 2010
Published 29 April 2010
Online at stacks.iop.org/JPhysA/43/205207

Abstract

We present a detailed calculation of the distance-dependent two-point function for quadrangulations with no multiple edges. Various discrete observables measuring this two-point function are computed and analyzed in the limit of large maps. For large distances and in the scaling regime, we recover the same universal scaling function as for general quadrangulations. We then explore the geometry of 'minimal neck baby universes' (minbus), which are the outgrowths to be removed from a general quadrangulation to transform it into a quadrangulation with no multiple edges, the 'mother universe'. We give a number of distance-dependent characterizations of minbus, such as the two-point function inside a minbu or the law for the distance from a random point to the mother universe.

PACS numbers: 02.10.Ox, 02.50.−r, 04.60.−m

(Some figures in this article are in colour only in the electronic version)

1. Introduction

1.1. The problem

The study of random maps is an active field of research which raises beautiful combinatorial and probabilistic problems. In particular, maps are used in physics as discrete models for fluctuating surfaces in a wide range of domains, like the study of biological membranes or string theory. Random maps can be equipped with statistical models, such as Ising spins, dimers, hard particles, and give rise to a large variety of critical phenomena, described in the physics literature by the so-called two-dimensional quantum gravity [1, 2]. For large maps, several sensible scaling limits of continuous surfaces can be reached, depending on the universality class of the model at hand. Of particular interest is the so-called Brownian map [3, 4], which describes the scaling limit of large non-critical planar maps (in the universality

class of the so-called pure gravity), like maps with prescribed face degrees, for instance planar triangulations (maps with faces of degree 3 only) or planar quadrangulations (maps with faces of degree 4 only).

The Brownian map was shown to have the topology of the two-dimensional sphere [5, 6], but it has nevertheless surprising geometrical properties, which place it half-way between a tree-like object and a smooth surface. For instance, it was shown that, as would happen in a tree, two geodesic paths leading to a given point in the map merge into a common geodesic before reaching this point. This is the so-called *confluence phenomenon* [7], which reveals some underlying tree-like structure of the Brownian map. On the other hand, it was shown that the triangle formed by three geodesic paths linking three points in the map delimit two macroscopic (interior and exterior) regions, like in a smooth surface [8, 9]. Heuristically, it was claimed that large maps can be viewed as made of a large component, the 'mother universe' with attached small components, the 'baby universes' arranged into tree-like structures (see for instance [10]). A proper definition of mother and baby universes is however lacking so far, which prevents from making this statement more precise.

Besides this qualitative picture of the Brownian map, precise quantitative measures of its geometry could be obtained, such as the two-point function [11–13], which gives the profile of distances between two random points in the map, and the three-point function [8], which gives the joint law for the three distances between three random points. In particular, the two- and three-point functions could be computed exactly at the discrete level in the context of general planar quadrangulations. Here, by general quadrangulations, we mean all maps with faces of degree 4 only. These maps cannot have loops (since they are clearly bipartite), but they may have *multiple edges*, creating cycles of length 2. Each of these cycles acts as a neck separating the quadrangulation into two components. Now we may imagine cutting the map along all its cycles of length 2, thus disconnecting it into several pieces. It was shown [14, 15] that, for quadrangulations with a large number n of faces, exactly one of these pieces has a size (= number of faces) of order n, while all the others have sizes negligible with respect to n. This provides a proper definition of a mother and a baby universe: the large component constitutes the mother universe. Upon gluing each of the cut cycles touching this component into a single edge, the mother universe may itself be viewed as a planar quadrangulation which, by construction, has no multiple edges. The other pieces, once reglued together, form a number of connected branched structures, each with a boundary of length 2. Each of these branched structures constitutes a baby universe, to be glued by its boundary to the mother universe to complete the quadrangulation.

It is well known that general planar (rooted) quadrangulations with n faces are in one-to-one correspondence with (rooted) general planar maps with n edges. Under this equivalence, the above decomposition of quadrangulations simply corresponds to the well-known decomposition of general maps into 2-connected components upon splitting them at their separating vertices.

It is clear that we have here a very restrictive definition of baby universes, the so-called *minimal neck baby universes* [16], hereafter abbreviated into *minbus* and corresponding to cutting the map along necks of minimal size 2. Unfortunately, the overlaps between cycles of larger sizes prevent from defining a canonical decomposition into more general baby universes.

Rather than considering general quadrangulations, we may at first start with the more restricted class of quadrangulations with no multiple edges (in one-to-one correspondence with 2-connected maps via the above-mentioned equivalence). These quadrangulations have no cycles of length 2 by definition, hence are reduced to their mother universe, with no minbus. It is expected that, for large distances, the two- and three-point functions of these

quadrangulations with no multiple edges be essentially the same as those of general maps since the presence of minbus should affect only small distances.

The purpose of this paper is twofold. In a first part, we present a detailed calculation of the *two-point function for quadrangulations with no multiple edges*. Expressions are given for various observables measuring this two-point function at the discrete level and then analyzed in the limit of large maps. Although different from that of general quadrangulations at finite distances, they give the same two-point function at large distances and in particular in the universal scaling regime. In a second part, we use the connection between general quadrangulations and quadrangulations with no multiple edges inherited from the above decomposition into the mother universe and minbus to explore a number of *distance-dependent characterizations of the minbus* themselves in general quadrangulations. We compute for instance the *two-point function inside a minbu* or the law for the distance from a random point to the mother universe.

The paper is organized as follows. In the second part of section 1, we recall the known results on the two-point function for general quadrangulations. These results are based on the Schaeffer bijection which encodes quadrangulations by the so-called well-labeled trees. In section 2.1 we introduce the more restricted family of *well-balanced* trees which code for quadrangulations with no multiple edges. Generating functions for these well-balanced trees are then computed either directly by solving the appropriate recursion relation (section 2.2) or indirectly via a substitution procedure relating them to generating functions for regular well-labeled trees (section 2.3). We end section 2 by deriving expressions for various quantities measuring, at the discrete level, the two-point function of quadrangulations with no multiple edges (section 2.4). These results are used in section 3 to address various questions on the two-point distance statistics. We first give explicit enumerations for small distances and small sizes in section 3.1, and discuss in section 3.2 the case of finite distances in quadrangulations of large size n (the local limit). We then explore in section 3.3 the scaling limit of large distances ($\propto n^{1/4}$) in large quadrangulations and recover the universal two-point function of the Brownian map. Section 4 is devoted to the study of minbus in general quadrangulations. We first recall in section 4.1 how to cut a general quadrangulation along minimal necks so as to decompose it into a mother universe and minbus. We then explain in section 4.2 the precise meaning of our generating functions for well-balanced trees in this context. We finally obtain in section 4.3 a number of distance-dependent properties of minbus such as the probability for two points to lie in the same minbu as a function of their mutual distance as well as the two-point function inside a minbu. The law for the distance to the mother universe or for the number of necks to go through to reach it is derived in the appendix. We end this paper by a few concluding remarks in section 5.

1.2. General quadrangulations and well-labeled trees: reminders

In the case of general quadrangulations, a fruitful approach to questions on the distance statistics relies on the Schaeffer bijection between quadrangulations and well-labeled trees [17]. It consists in a one-to-one coding of *pointed* (i.e. with a marked vertex called the *origin*) quadrangulations with n faces by *well-labeled trees* with n edges, i.e. plane trees whose vertices carry integer labels subject to the two conditions:

(i) the labels of two vertices adjacent in the tree differ by at most 1;
(ii) the minimum label is 1.

The $n+1$ vertices of the well-labeled tree are in one-to-one correspondence with the $(n+2)-1$ vertices of the quadrangulation other than the origin, and the label of a vertex in the tree is nothing but the distance from the associated vertex to the origin in the quadrangulation.

Moreover, the $2n$ corners of the tree are in one-to-one correspondence with the $2n$ edges of the quadrangulation. By *corner*, we mean the angular sector between two consecutive edges around a vertex of the tree, and if that vertex has label ℓ we also say that the corner has label ℓ. The corners with label ℓ in the tree are in one-to-one correspondence with the edges of type $(\ell-1)\to\ell$ in the quadrangulation, i.e. the edges connecting a vertex at distance $(\ell-1)$ from the origin to a vertex at distance ℓ. Finally, the edges of the tree are in one-to-one correspondence with the faces of the quadrangulation.

A *planted* tree is a (plane) tree with a marked corner whose label is called the root label. It is also convenient to introduce *almost well-labeled trees* where condition (ii) is released into:

(ii)′ the minimum label is larger than or equal to 1.

Attaching a weight g per edge, the generating function $R_\ell \equiv R_\ell(g)$ of planted almost well-labeled trees with root label ℓ satisfies the recursion relation:

$$R_\ell = \frac{1}{1-g(R_{\ell-1}+R_\ell+R_{\ell+1})} \tag{1.1}$$

for $\ell \geqslant 1$, with the initial condition $R_0 = 0$. This relation simply states that a tree with root label ℓ is fully characterized by the sequence of its descending subtrees, which are themselves planted almost well-labeled trees with root label $(\ell-1)$, ℓ or $(\ell+1)$. Equation (1.1) implies in particular the conservation law:

$$C_{\ell+1} = C_\ell \qquad \text{with} \qquad C_\ell \equiv R_\ell - gR_{\ell-1}R_\ell R_{\ell+1}, \tag{1.2}$$

which may also be derived combinatorially [18]. Writing $C_\ell = C_\infty$ leads after some simple manipulations to the explicit solution [13]:

$$R_\ell = R\frac{(1-x^\ell)(1-x^{\ell+3})}{(1-x^{\ell+1})(1-x^{\ell+2})}$$

$$\text{where} \quad R = \frac{1-\sqrt{1-12g}}{6g} \qquad \text{and} \qquad x+\frac{1}{x}+1 = \frac{1}{gR^2}. \tag{1.3}$$

Here, we introduced the quantity $R \equiv \lim_{\ell\to\infty} R_\ell$, solution of the quadratic equation $R = 1 + 3g\,R^2$. Of particular interest is the case $\ell = 1$ for which conditions (ii) and (ii)′ coincide so that R_1 is the generating function of well-labeled trees with a marked corner with label 1. From Schaeffer's bijection, this is also the generating function of *rooted* (i.e. with a marked oriented edge) quadrangulations with a weight g per face. Writing $C_1 = C_\infty$ gives

$$R_1 = R - gR^3. \tag{1.4}$$

If we now wish to address the question of the two-point function, i.e. the law for the distance between two 'points' (edges or vertices) picked at random in quadrangulations, this can be done by considering several possible distance-dependent generating functions. For instance, we may consider pointed quadrangulations with, in addition to their marked origin vertex, a marked edge of type $(\ell-1)\to\ell$ with respect to this origin. Let us denote by $Q_\ell \equiv Q_\ell(g)$ the corresponding generating function with a weight g per face. In the tree language, it enumerates planted well-labeled trees with root label ℓ. This leads immediately to

$$Q_\ell = R_\ell - R_{\ell-1} \tag{1.5}$$

since condition (ii) is easily restored from condition (ii)′ by eliminating the configurations (with root label ℓ) having a minimum label strictly larger than 1, counted by $R_{\ell-1}$ by a simple shift of labels.

Another measure of the two-point distance statistics is via the generating function F_ℓ of rooted quadrangulations having, in addition to their marked oriented root edge, a marked

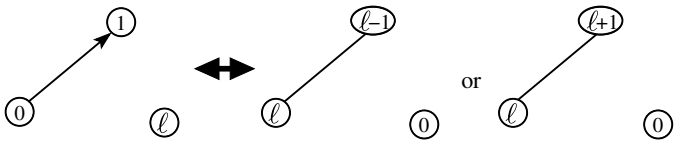

Figure 1. A schematic picture of the re-rooting procedure, showing that there is a bijection between, on the one hand, rooted maps with a marked vertex at distance ℓ from the origin of the root edge and, on the other hand, pointed maps with a marked edge of type $(\ell-1)\to\ell$ or $\ell\to(\ell+1)$ with respect to the origin vertex.

vertex at distance ℓ from the origin of the root edge. In the tree language, F_ℓ is the generating function of planted well-labeled trees with a root vertex with label 1 and with an extra marked vertex with label ℓ. The tree then consists of a chain of almost well-labeled trees attached on both sides of a linear spine linking these two vertices. Only one subtree with root label ℓ is attached at the endpoint of the spine. We shall call these configurations *vertex-ended chains* and their generating function reads

$$F_\ell = \left\{ \sum_{k\geqslant 0} \sum_{\substack{\text{paths } (1=\ell_0,\ell_1,\ldots,\ell_k=\ell)\\ \ell_i\geqslant 1,\ |\ell_i-\ell_{i-1}|\leqslant 1, i=1,\ldots,k}} \prod_{i=0}^{k-1} g(R_{\ell_i})^2 \right\} \times R_\ell \tag{1.6}$$

where k is the length of the spine.

Now, by a simple re-rooting procedure, there is a clear bijection between maps with a marked root edge and a marked vertex at distance ℓ from the origin of the root edge, and maps with a marked origin and a marked edge of type $(\ell-1)\to\ell$ or of type $\ell\to(\ell+1)$ with respect to this origin (see figure 1 for an illustration). This bijection translates into the simple relation

$$F_\ell = Q_\ell + Q_{\ell+1} = R_{\ell+1} - R_{\ell-1} \tag{1.7}$$

for $\ell\geqslant 1$, a formula which can also be obtained directly by induction from (1.6) by use of the conservation law.

Finally, a third interesting measure of the two-point distance statistics is via the generating function H_ℓ of rooted quadrangulations having, in addition to the marked oriented root edge, an extra marked edge of type $(\ell-1)\to\ell$ with respect to the origin of the root edge (if $\ell=1$, we may choose for the extra marked edge the root edge itself, in which case the configuration is counted with a weight 2 for convenience). In terms of trees, this amounts to replacing the marked vertex with label ℓ in the configurations counted by F_ℓ by a marked corner. This leads to the same chain of almost well-labeled trees as for F_ℓ, with now two trees with label ℓ instead of one attached to the endpoint of the spine. We shall call these configurations *corner-ended chains* and their generating function reads

$$H_\ell = R_\ell\ F_\ell = R_{\ell+1}\ R_\ell - R_\ell\ R_{\ell-1} \tag{1.8}$$

for $\ell\geqslant 1$.

The generating functions Q_ℓ, F_ℓ and H_ℓ, although clearly different, are equivalently good measures of the two-point function at the discrete level. In the limit of quadrangulations with a large number n of faces and for large distances (of order $n^{1/4}$), they lead to the same distance statistics, characterized by a unique scaling function, the (universal) continuous two-point function.

2. Quadrangulations with no multiple edges and well-balanced well-labeled trees

We now turn to the study of quadrangulations with no multiple edges, i.e. quadrangulations where *all pairs of vertices are linked by at most one edge*. As already mentioned, these (rooted) quadrangulations with n faces are in one-to-one correspondence with (rooted) general maps with n edges *having no separating vertex*. Such maps are usually called 2-connected or nonseparable and were first enumerated in [19–21]. More recently, a bijection between nonseparable maps and two different families of trees was discovered in [22], which explains the remarkably simple formula for their number. These trees are (1) so-called *description trees* which are a particular class of labeled trees (with arbitrary internal degrees) and (2) so-called *skew ternary trees* which are ternary trees with particular positivity constraints.

If the enumeration of quadrangulations with no multiple edges is a well-understood question, much less is known on their distance statistics. Here we shall present yet another bijection with labeled trees, obtained by simply restricting the general class of well-labeled trees in the Schaeffer bijection to a smaller class of *well-balanced* ones where additional constraints guarantee that the associated quadrangulation has no multiple edges. Even if it seems likely that a direct correspondence can be found between these trees and the description trees of [22], well-balanced trees are particularly adapted to questions involving the distance and this is the reason why we use them here.

2.1. Well-balanced well-labeled trees

Before we address the question of multiple edges, let us recall how we obtain a pointed quadrangulation from its associated well-labeled tree in the Schaeffer bijection. First we take for the vertices of the quadrangulation all the vertices of the tree plus an extra added vertex with label 0, which will be the origin of the quadrangulation. The edges of the quadrangulation are then obtained by connecting each *corner* of the tree with label ℓ to its *successor*, which is the first corner at a vertex with label $\ell - 1$ encountered clockwise around the tree if $\ell > 1$, or the added vertex with label 0 if $\ell = 1$. These connections can be performed without edge crossings. We finally erase all the original tree edges as well as the vertex labels.

It is now straightforward to deduce under which condition the quadrangulation will have no multiple edges. First, as any corner at a vertex with label 1 will be linked to the origin, the absence of multiple edges requires that there is exactly one corner at any vertex with label 1 (see figure 2(*a*) for a counterexample), namely that:

(a) vertices with label 1 are leaves of the tree.

Consider now a vertex with label $\ell > 1$, which we assume is not a leaf of the tree, and consider two successive corners clockwise around this vertex. Multiple edges will appear in the quadrangulation if these two corners have the same successor. This occurs if the subtree attached to the considered vertex and lying between the two considered corners does not contain any vertex with label $\ell - 1$ (see figure 2(*b*)). A necessary and sufficient condition for the absence of multiple edges of type $\ell \to (\ell - 1)$ is that:

(b) each of the k subtrees attached to a vertex of degree k in the tree and with label $\ell > 1$ contains a vertex with label $\ell - 1$.

Note that this condition is automatically satisfied if the vertex is a leaf ($k = 1$) with label $\ell > 1$ as the only attached subtree is then the entire tree itself (minus the considered vertex) which, from (i) and (ii), contains all integer labels between 1 and ℓ.

A well-labeled tree satisfying (a) and (b) will be called *well-balanced*. We have a bijection between pointed quadrangulations with n faces and with no multiple edges and well-balanced well-labeled trees with n edges.

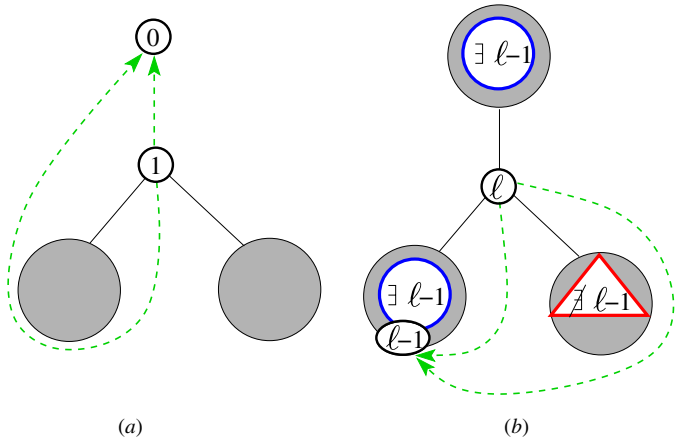

Figure 2. A schematic picture for the appearance of a double edge when reconstructing a quadrangulation from its associated well-labeled tree. A double edge is found either (*a*) when a vertex with label 1 is not a leaf or (*b*) when the subtree separating two given successive corners at a vertex with label $\ell > 1$ contains no label $(\ell - 1)$.

2.2. Generating functions for almost well-balanced trees and enumeration of quadrangulations with no multiple edges

As in section 1.2, let us slightly modify the label constraints on the trees so as to get simpler generating functions. Let us define *almost well-balanced well-labeled trees* as planted trees which are almost well-labeled, i.e. carry integer vertex labels satisfying (i) and (ii)′ above, and are also almost well-balanced, i.e. satisfy the conditions:

(a)′ vertices with label 1 have no *descending* subtrees.
(b)′ any *descending* subtree attached to a vertex with label $\ell' > 1$ in the tree contains a vertex with label $(\ell' - 1)$.

We denote by $r_\ell \equiv r_\ell(z)$ the generating function of these trees with root label ℓ and with a weight z per edge. If $\ell > 1$, condition (a)′ is equivalent to (a) but (b)′ is weaker than (b) as we do not impose any constraint on the ascending subtrees. Therefore, almost well-balanced trees are not well-balanced in general. When $\ell = 1$, i.e. when the root label itself is 1, (a)′ implies drastically that the whole tree reduces to a single vertex with label 1, with the trivial generating function

$$r_1 = 1. \tag{2.1}$$

This is to be contrasted with the generating function $p_1 \equiv p_1(z)$ of the truly well-balanced well-labeled trees planted at a vertex with label 1. This generating function, which is also that of *rooted* quadrangulations with no multiple edges with a weight z per face, can be obtained as follows. From (a), the root vertex in this case is necessarily a leaf and either the tree reduces to two leaves with label 1 connected by a single edge (see figure 3(*a*)) or the tree is made of a leaf with label 1 connected by an edge to an almost well-labeled tree planted at a vertex with label 2 (see figure 3(*b*)). It is enough to demand that this attached tree be almost well-balanced as, if so, the entire tree is well-balanced. This is because condition (b) is also clearly satisfied for ascending subtrees in this case, due to the existence of label 1 at the top of the tree, which, from (i), ensures that any vertex with label $\ell > 1$ has an ancestor vertex in the tree with label

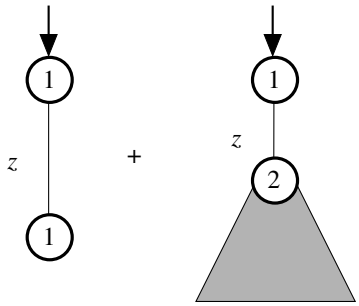

Figure 3. A schematic picture of the relation $p_1 = z(1 + r_2)$ for the generating function p_1 of well-balanced well-labeled trees planted at a vertex with label 1. This vertex is necessarily a leaf, linked either to another leaf with label 1 or to an almost well-balanced well-labeled tree with root label 2, represented here by a gray triangle.

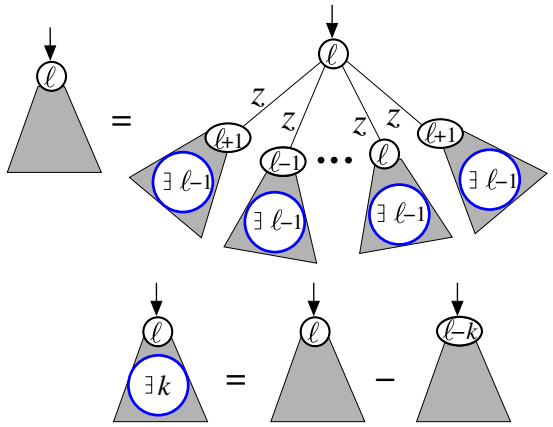

Figure 4. Top: a schematic picture of relation (2.3) for the generating function r_ℓ of almost well-balanced well-labeled trees with root label ℓ. Any such tree is entirely specified by the sequence of its descending subtrees (gray triangles), which are themselves almost well-balanced well-labeled trees with root label $(\ell - 1)$, ℓ or $(\ell + 1)$. Each of these subtrees must contain a vertex with label $(\ell - 1)$. Bottom: a schematic representation of relation (2.4).

$(\ell - 1)$. To summarize, the generating function of rooted quadrangulations with no multiple edges reads

$$p_1 = z + zr_2. \tag{2.2}$$

Let us now derive an explicit expression for the generating functions r_ℓ. It may be obtained in two different ways: we may either get it as the solution of some recursion relation of the type (1.1), now incorporating the constraint of having almost well-balanced trees. This approach is presented in detail in this section. Or, as explained in the next section, we may obtain it directly from the explicit form (1.3) of R_ℓ via a simple substitution procedure.

The generating functions r_ℓ obey the following relation for $\ell \geqslant 1$, illustrated in figure 4:

$$r_\ell = \frac{1}{1 - z\left(r_{\ell-1}^{(\ell-1)} + r_\ell^{(\ell-1)} + r_{\ell+1}^{(\ell-1)}\right)} \tag{2.3}$$

where we introduced the generating function $r_\ell^{(k)}$ $(0 \leqslant k \leqslant \ell)$ for almost well-balanced well-labeled trees planted at a vertex with label ℓ and satisfying the extra requirement that they contain a vertex with label k. Equation (2.3) simply states that an almost well-balanced well-labeled tree with root label ℓ may be viewed as a sequence of almost well-balanced well-labeled subtrees with root label $(\ell-1)$, ℓ or $(\ell+1)$, each of them containing a vertex with label $(\ell-1)$.

Now any almost well-balanced well-labeled tree with root label ℓ and with no occurrence of the label $k \leqslant \ell$ has all its labels strictly larger than k. Shifting all labels by k creates a tree which is still almost well-balanced and almost well-labeled, and now has root label $\ell - k$. This leads to the relation

$$r_\ell^{(k)} = r_\ell - r_{\ell-k} \tag{2.4}$$

with $r_0 = 0$. We have in particular $r_{\ell-1}^{(\ell-1)} = r_{\ell-1}$ since a label $(\ell-1)$ is already present at the level of the root, $r_\ell^{(\ell-1)} = r_\ell - r_1 = r_\ell - 1$ since a label $(\ell-1)$ is automatically present in each subtree and therefore the only situation with no label $(\ell-1)$ is when the tree reduces to its root vertex. Finally, we have $r_{\ell+1}^{(\ell-1)} = r_{\ell+1} - r_2$ so that equation (2.3) translates into the recursion relation

$$r_\ell = \frac{1}{1 - z(r_{\ell-1} + r_\ell + r_{\ell+1}) + z(r_1 + r_2)} \tag{2.5}$$

valid for all $\ell \geqslant 1$. Taking $\ell \to \infty$ gives

$$r \equiv \lim_{\ell\to\infty} r_\ell = \frac{1}{1 - 3zr + z + zr_2} \tag{2.6}$$

namely

$$r_2 = 3r - 1 + \frac{1-r}{zr}. \tag{2.7}$$

Writing (2.5) for ℓ and $\ell+1$ as

$$\begin{aligned} 1 &= r_\ell(1 + z(r_1 + r_2)) - zr_\ell(r_{\ell-1} + r_\ell + r_{\ell+1}) \\ 1 &= r_{\ell+1}(1 + z(r_1 + r_2)) - zr_{\ell+1}(r_\ell + r_{\ell+1} + r_{\ell+2}), \end{aligned} \tag{2.8}$$

multiplying the first line by $r_{\ell+1}$, the second line by r_ℓ and taking the difference leads to the conservation property

$$c_{\ell+1} = c_\ell \qquad \text{with} \qquad c_\ell \equiv r_\ell - zr_{\ell-1}r_\ell r_{\ell+1} \tag{2.9}$$

Alternatively, this conservation property may be obtained by the same combinatorial argument as that for general well-labeled trees [18]: let us consider planted almost well-balanced well-labeled trees having root label ℓ and *containing a vertex with label 1*. By definition, their generating function is $r_\ell^{(1)}$. But also any such tree can be decomposed into three parts as follows. In the sequence of subtrees attached to the root, let us single out the leftmost one containing a label 1, which is the first part in our decomposition. The second (resp. third) part is formed by all subtrees on its left (resp. right) together with the root vertex. It is easily seen that the three parts are planted almost well-balanced well-labeled trees. Moreover, the first part has root label $\ell-1$, ℓ or $\ell+1$ and necessarily contains a label 1, the second part contains no label 1 (therefore by shifting all labels by 1 we obtain a tree with root label $\ell-1$) and finally the third tree has the root label ℓ and obeys no further constraint. Clearly this

decomposition is reversible and the total number of edges is decreased by one, leading to the relation

$$r_\ell^{(1)} = z\big(r_{\ell-1}^{(1)} + r_\ell^{(1)} + r_{\ell+1}^{(1)}\big)\, r_{\ell-1} r_\ell, \tag{2.10}$$

which, together with (2.4), immediately implies the conservation property (2.9).

We now deduce that $c_\ell = c_1 = 1$ for all $\ell \geqslant 1$, namely

$$r_\ell = 1 + z r_{\ell-1} r_\ell r_{\ell+1} \tag{2.11}$$

and in particular

$$r = 1 + z r^3 \tag{2.12}$$

or explicitly

$$r = \frac{2}{\sqrt{3z}} \sin\left(\frac{1}{3}\arcsin\sqrt{\frac{27z}{4}}\right) = \sum_{n\geqslant 0} \frac{(3n)!}{(2n+1)!n!} z^n. \tag{2.13}$$

From (2.7), we deduce that

$$r_2 = 3r - 1 - r^2 = 1 + \sum_{n\geqslant 1} \frac{2(3n)!}{(2n+1)!(n+1)!} z^n. \tag{2.14}$$

From (2.2), the generating function p_1 finally reads

$$p_1 = zr(3-r) = \sum_{n\geqslant 1} \frac{2(3n-3)!}{(2n-1)!n!} z^n \tag{2.15}$$

from which we read off the number of rooted quadrangulations with n faces and with no multiple edges [19–21]. Here we observe a connection with the formulation of [22] by noting that r (respectively p_1) is precisely the generating function for ternary (respectively skew ternary) trees.

The conservation law (2.9) is identical to that, (1.2), of general well-labeled trees and only the precise value of the conserved quantity differs (1 instead of R_1). Repeating the manipulations leading from (1.2) to the explicit form (1.3), we immediately deduce from the new conservation law (2.9) the form of r_ℓ for general ℓ:

$$r_\ell = r\frac{(1-y^\ell)(1-y^{\ell+3})}{(1-y^{\ell+1})(1-y^{\ell+2})} \tag{2.16}$$

with r as above and $y \equiv y(z)$ solution of

$$y + \frac{1}{y} + 1 = \frac{1}{zr^2}. \tag{2.17}$$

2.3. Approach by substitution

Rather than solving the recursion relation (2.5), we may alternatively recover the above expression for r_ℓ, as well as all the results in section 2.2, directly from the known form (1.3) of R_ℓ via a substitution procedure as follows.

Starting with an almost well-labeled tree planted at a vertex with label ℓ, as counted by R_ℓ, we may realize conditions (a)′–(b)′ by simply erasing all descending subtrees attached to vertices with label 1 and, at each vertex with label $\ell' > 1$, erase any of its descending subtrees which does not contain a label $\ell' - 1$. The remaining tree is clearly an almost well-balanced well-labeled tree, counted by r_ℓ. Conversely, we recover a general almost well-labeled tree from an almost well-balanced well-labeled one by attaching *at each corner* with label $\ell' \geqslant 1$

an arbitrary well-labeled subtrees with root label ℓ' and with no label $\ell'-1$, i.e. with all its labels larger than or equal to ℓ'. Any such subtree is counted by R_1, independently of ℓ', as obtained by shifting all labels by $\ell'-1$. For a planted tree with n edges, there are exactly $2n+1$ corners where to attach the subtrees. This results into the identity

$$R_\ell(g) = R_1(g) r_\ell(g(R_1(g))^2). \tag{2.18}$$

Introducing the function $z(g)$ defined as

$$z(g) \equiv g\ (R_1(g))^2 \tag{2.19}$$

and its inverse function $g(z)$, we may write (2.18) as

$$r_\ell(z) = \frac{R_\ell(g(z))}{R_1(g(z))} \qquad \text{and in particular} \qquad r(z) = \frac{R(g(z))}{R_1(g(z))}. \tag{2.20}$$

Using $R_1 = R - gR^3$, we may write $R/R_1 = 1 + gR_1^2(R/R_1)^3$ for $g = g(z)$, leading to the characterization $r = 1 + zr^3$ of $r \equiv r(z)$, which matches the characterization (2.12) of the previous section. Combining (2.19) and (2.20), we deduce that

$$zr(z)^2 = g(z)R((g(z))^2 \tag{2.21}$$

so that if $x = x(g)$ is the solution of $x + 1/x + 1 = 1/(gR^2)$, then $y \equiv y(z) = x(g(z))$ is the solution of $y + 1/y + 1 = 1/(zr^2)$, while (2.20) gives explicitly

$$r_\ell(z) = \frac{R(g(z))}{R_1(g(z))}\ \frac{(1-(x(g(z))^\ell)(1-(x(g(z))^{\ell+3})}{(1-(x(g(z))^{\ell+1})(1-(x(g(z))^{\ell+2})} = r\frac{(1-y^\ell)(1-y^{\ell+3})}{(1-y^{\ell+1})(1-y^{\ell+2})} \tag{2.22}$$

which is precisely expression (2.16).

2.4. Two-point function for quadrangulation with no multiple edges

In the case of general quadrangulations, we could easily go from almost well-labeled trees (as counted by R_ℓ) to fully well-labeled ones (as counted by Q_ℓ, F_ℓ or H_ℓ). Using (1.5), (1.7) or (1.8), we could extract from (1.3) explicit expressions for the various discrete versions of the two-point function. For quadrangulations with no multiple edges, we may again restore condition (ii) of well-labeled trees from condition (ii)$'$ of almost well-labeled ones by considering the analog of Q_ℓ, i.e. the generating function $q_\ell \equiv q_\ell(z)$ defined as

$$q_\ell = r_\ell - r_{\ell-1}. \tag{2.23}$$

Unfortunately, the trees counted by q_ℓ are in general not well-balanced and restoring condition (b) from condition (b)$'$ is not so simple as it requires considering ascending subtrees. As such, the knowledge of r_ℓ or q_ℓ is not directly sufficient to answer the question of the two-point function.

Fortunately, we may circumvent this problem by considering instead the analogs of the generating functions F_ℓ and H_ℓ in section 1.2.

More precisely, as in (1.6), we define the generating function $f_\ell \equiv f_\ell(z)$ for *almost well-balanced vertex-ended chains* as

$$f_\ell = \left\{ \sum_{k\geqslant 0} \sum_{\substack{\text{paths } (1=\ell_0,\ell_1,\dots,\ell_k=\ell) \\ \ell_i\geqslant 1,\ |\ell_i-\ell_{i-1}|\leqslant 1, i=1,\dots,k}} \prod_{i=0}^{k-1} z(r_{\ell_i})^2 \right\} \times r_\ell \tag{2.24}$$

and the generating function $h_\ell \equiv h_\ell(z)$ for *almost well-balanced corner-ended chains*:

$$h_\ell = r_\ell f_\ell \tag{2.25}$$

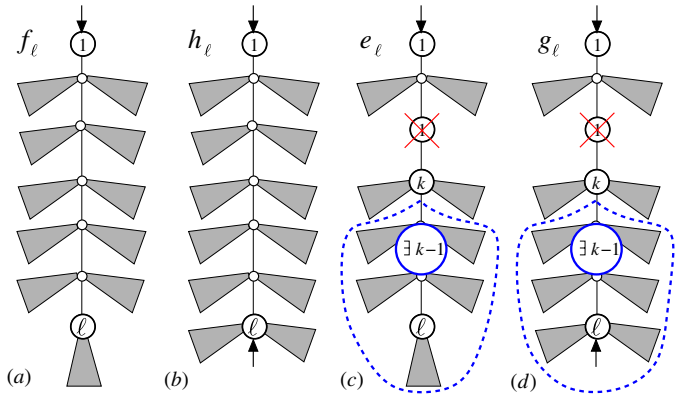

Figure 5. A schematic picture of the generating functions f_ℓ, h_ℓ, e_ℓ and g_ℓ for chains of almost well-balanced well-labeled trees. The end of the chain is either a marked vertex with label ℓ (in f_ℓ or e_ℓ) or a marked corner with label ℓ (in h_ℓ or g_ℓ). We ensure that the trees enumerated by g_ℓ or e_ℓ are fully well-balanced by forbidding the appearance of label 1 along the spine of the chain and by demanding that, for each vertex with label k along the spine, the subtree formed by the part of the spine lying strictly below this vertex and by the attached subtrees contains a label $(k-1)$.

with one extra subtree with root label ℓ (see figures 5(*a*) and (*b*) for an illustration). The generating function f_ℓ satisfies the recursion

$$f_\ell = \delta_{\ell,1} + z r_\ell (f_{\ell-1} r_{\ell-1} + f_\ell r_\ell + f_{\ell+1} r_{\ell+1}) \tag{2.26}$$

with $f_0 = 0$, which determines all f_ℓ with $\ell \geqslant 1$ as power series in z from the initial condition $f_\ell = z^{\ell-1} + \mathcal{O}(z^\ell)$. Writing the conservation law (2.9) as $c_{\ell+1} = c_{\ell-1} + \delta_{\ell,1}$ (this form is also valid when $\ell = 1$), we have

$$\begin{aligned} r_{\ell+1} - r_{\ell-1} &= \delta_{\ell,1} + z r_\ell (r_{\ell+1} r_{\ell+2} - r_{\ell-1} r_{\ell-2}) \\ &= \delta_{\ell,1} + z r_\ell (r_{\ell+1}(r_{\ell+2} - r_\ell) + r_\ell (r_{\ell+1} - r_{\ell-1}) + r_{\ell-1}(r_\ell - r_{\ell-2})) \end{aligned} \tag{2.27}$$

from which we identify the solution of (2.26) as

$$f_\ell = r_{\ell+1} - r_{\ell-1} = r y^{\ell-1} \frac{(1-y)(1-y^2)^2(1-y^{2\ell+3})}{(1-y^\ell)(1-y^{\ell+1})(1-y^{\ell+2})(1-y^{\ell+3})} \tag{2.28}$$

while

$$h_\ell = r_{\ell+1} r_\ell - r_\ell r_{\ell-1} = r^2 y^{\ell-1} \frac{(1-y)(1-y^2)^2(1-y^{2\ell+3})}{(1-y^{\ell+1})^2(1-y^{\ell+2})^2}. \tag{2.29}$$

We therefore have the same relations (2.28) and (2.29) for the generating function of our chains of well-balanced trees in terms of r_ℓ as those (1.7) and (1.8) we had for general trees. This is not a surprise as, by a simple substitution argument as above, we may write directly

$$F_\ell(g) = R_1(g) f_\ell(g(R_1(g))^2), \qquad H_\ell(g) = (R_1(g))^2 h_\ell(g(R_1(g))^2) \tag{2.30}$$

so that (1.7) and (1.8) immediately translate into (2.28) and (2.29) upon taking $g = g(z)$.

The almost well-balanced chains above are not fully well-balanced trees in general, but this problem may now be cured by a simple inclusion–exclusion procedure. More precisely, in the trees counted by f_ℓ or h_ℓ, condition (b) is automatically satisfied for all ascending subtrees due to the presence of label 1 at the top of the tree which, from (i), guarantees that any vertex $\ell' > 1$ in the tree has an ancestor with label $\ell' - 1$. Since we attached almost well-balanced

subtrees to vertices of the spine, condition (b) is also satisfied for all descending subtrees *except possibly at vertices of the spine itself* and only for the descending subtree consisting of the part of the spine lying strictly below such a spine vertex, together with the attached subtrees (see figure 5 for an illustration). Similarly, condition (a) is satisfied everywhere except possibly along the spine where we may encounter bivalent vertices with label 1.

Let us denote by $e_\ell \equiv e_\ell(z)$ (respectively $g_\ell \equiv g_\ell(z)$) the generating function for fully *well-labeled vertex-ended chains* (respectively *well-labeled corner-ended chains*) with conditions (a) and (b) also satisfied along the spine (see figures 5(*c*) and (*d*) for an illustration). We explain below how to obtain e_ℓ and g_ℓ from f_ℓ and h_ℓ but let us first observe that, from the bijection of section 2.1, e_ℓ and g_ℓ are good generating functions for quadrangulations with no multiple edges. More precisely, e_ℓ is the generating function of *rooted* quadrangulations with no multiple edges with a weight z per face and, in addition to their marked oriented root edge, with a marked vertex at distance ℓ from the origin of the root edge. Similarly, g_ℓ is precisely the generating function of *rooted* quadrangulations with no multiple edges and in addition with their marked oriented root edge, with an extra marked edge of type $(\ell-1) \to \ell$, i.e. connecting a vertex at distance $\ell-1$ from the origin of the root edge to a vertex at distance ℓ.

These interpretations hold only for $\ell > 1$ while the case $\ell = 1$ requires more attention: for convenience, if $\ell = 1$, we decide *not to include* in $e_1 = g_1$ the contribution 1 corresponding to the trivial case where the spine (and consequently the entire tree) reduces to a single vertex with label 1. In other words, the spine is required to have a non-zero length. Returning to maps, this implies that e_1 counts rooted quadrangulations with no multiple edges having an extra marked vertex adjacent to the origin but *different from the endpoint of the root edge*. We may reinstate the missing configurations by considering the generating function $p_1 + e_1$ instead. Similarly, g_1 counts rooted quadrangulations with no multiple edges having an extra marked edge incident to the origin but *different from the root edge itself*. Again we may reinstate the missing configurations by considering $p_1 + g_1$.

Let us now relate e_ℓ and g_ℓ to f_ℓ and h_ℓ. By looking, in a configuration counted by h_ℓ, at the first 'unsatisfied' vertex along the spine, with label k, we deduce the relation, valid for $\ell > 1$,

$$h_\ell = g_\ell + \left(\sum_{k=1}^{\ell-1} g_k h_{\ell+1-k}\right) + g_\ell(h_1 - 1) \qquad (\ell > 1). \tag{2.31}$$

The first term corresponds to the case where there is no unsatisfied vertex, leading to the desired g_ℓ. The second term corresponds to a first unsatisfied vertex along the spine with label k between 1 and $\ell-1$: the part of the tree lying above the unsatisfied vertex (including the left and right subtrees attached to this vertex) has no unsatisfied vertex and final label k, hence is counted by g_k while the rest of the tree has no label $k-1$ and therefore has all its labels strictly larger than $k-1$. Upon shifting all labels by $k-1$, we get a tree whose root is a leaf with label 1 and whose final vertex at the end of the spine has label $\ell+1-k$, and hence a tree counted by $h_{\ell+1-k}$. This situation incorporates the case (when $k = 1$) of label 1 along the spine with an undesired descending subtree, counted by h_ℓ. The third term corresponds to having the first unsatisfied vertex with label ℓ, in which case we can repeat the above argument provided we make sure that the descending subtree is not empty, resulting in a factor $h_1 - 1$ instead of h_1. Finally, any vertex with label $k > \ell$ along the spine cannot be unsatisfied due to the presence of the vertex with label ℓ at the end of the spine, which implies that all intermediate values of labels appear in between along the spine. For $\ell = 1$, we have the relation

$$h_1 = 1 + g_1 h_1 \tag{2.32}$$

obtained by cutting a configuration counted by h_1 at the first label 1 encountered along the spine (and different from the root vertex). This relation, together with (2.31), can be summarized into

$$h_\ell = \delta_{\ell,1} + \sum_{k=1}^{\ell} g_k h_{\ell+1-k} \tag{2.33}$$

which allows us in principle to compute g_ℓ from the explicit form (2.29) of h_ℓ. Introducing a new parameter t conjugate to ℓ and the corresponding generating functions

$$\hat{h}(t,z) \equiv \sum_{\ell\geqslant 0} h_{\ell+1}(z)t^\ell, \qquad \hat{g}(t,z) \equiv \sum_{\ell\geqslant 0} g_{\ell+1}(z)t^\ell, \tag{2.34}$$

equation (2.33) may be equivalently written as

$$\hat{h}(t,z) = 1 + \hat{g}(t,z)\hat{h}(t,z), \qquad \text{i.e.} \qquad \hat{g}(t,z) = 1 - \frac{1}{\hat{h}(t,z)}. \tag{2.35}$$

As for e_ℓ, we have the relation, valid for $\ell > 1$,

$$f_\ell = e_\ell + \left(\sum_{k=1}^{\ell-1} g_k f_{\ell+1-k}\right) + g_\ell(f_1 - 1) \qquad (\ell > 1) \tag{2.36}$$

obtained again by looking at the first unsatisfied vertex along the spine in a configuration counted by f_ℓ. For $\ell = 1$, we have instead $f_1 = 1 + g_1 f_1$ while $e_1 = g_1$. We may therefore write $f_1 = 1 + (e_1 - g_1) + g_1 f_1$ which can be summarized with (2.36) into

$$f_\ell = \delta_{\ell,1} + (e_\ell - g_\ell) + \sum_{k=1}^{\ell} g_k f_{\ell+1-k}. \tag{2.37}$$

Introducing again

$$\hat{f}(t,z) \equiv \sum_{\ell\geqslant 0} f_{\ell+1}(z)t^\ell, \qquad \hat{e}(t,z) \equiv \sum_{\ell\geqslant 0} e_{\ell+1}(z)t^\ell \tag{2.38}$$

we may rewrite (2.37) as

$$\hat{f}(t,z) = 1 + (\hat{e}(t,z) - \hat{g}(t,z)) + \hat{f}(t,z)\hat{g}(t,z), \qquad \text{i.e.} \quad \hat{e}(t,z) = \frac{\hat{f}(t,z) - 1}{\hat{h}(t,z)} \tag{2.39}$$

where we used (2.35) to eliminate $\hat{g}(t,z)$. This again allows us in principle to compute e_ℓ from the explicit forms (2.28) and (2.29) of f_ℓ and h_ℓ.

Let us end this section by considering the generating function $p_\ell \equiv p_\ell(z)$ of *pointed* quadrangulations with no multiple edges, with a weight z per face and with, in addition to their marked origin vertex, a marked edge of type $(\ell - 1) \to \ell$ with respect to this origin. As we already discussed, we may exchange the role of the marked vertices and edges (see figure 1 for an illustration), so that we may write

$$e_\ell = p_\ell + p_{\ell+1} \qquad (\ell > 1) \tag{2.40}$$

while, for $\ell = 1$, we have $e_1 = p_2$ since we imposed in the configurations counted by e_1 that the marked vertex be different from the endpoint of the root edge; hence, the marked vertex is at distance 2 from this endpoint. Recall finally that p_1 counts rooted quadrangulations. Introducing

$$\hat{p}(t,z) \equiv \sum_{\ell\geqslant 0} p_{\ell+1}(z)t^\ell \tag{2.41}$$

we may summarize the above relations into

$$\hat{e}(t,z) = e_1(z) + \hat{p}(t,z) - p_1(z) + \frac{\hat{p}(t,z) - tp_2(z) - p_1(z)}{t},$$

$$\text{i.e.} \quad \hat{p}(t,z) = p_1(z) + \frac{t}{1+t}\,\hat{e}(t,z) = p_1(z) + \frac{t}{1+t}\,\frac{\hat{f}(t,z)-1}{\hat{h}(t,z)} \tag{2.42}$$

with p_1 as in (2.15).

Note that in the same way as e_ℓ and g_ℓ are the fully well-balanced counterparts of f_ℓ and h_ℓ, p_ℓ may be viewed as the fully well-balanced counterpart of q_ℓ. Writing $f_\ell = q_\ell + q_{\ell+1}$, we may, after some simple algebra, rewrite (2.42) as

$$\hat{p}(t,z) = p_1(z) + \frac{\hat{q}(t,z)-1}{\hat{h}(t,z)} \qquad \text{with} \qquad \hat{q}(t,z) \equiv \sum_{\ell \geqslant 0} q_{\ell+1} t^\ell. \tag{2.43}$$

3. Distance statistics in large quadrangulations with no multiple edges

3.1. Simple enumerations

As a non-trivial check of the formulas in section 2.4, we may verify some sum rules by computing $\hat{e}(1,z)$, $\hat{g}(1,z)$ and $\hat{p}(1,z)$ which correspond to quadrangulations with two marked 'points' (vertices or edges) without constraint on the distance. Using $\sum_{\ell=1}^{\ell_{\max}} f_\ell = r_{\ell_{\max}+1} + r_{\ell_{\max}} - r_1$, we deduce that

$$\hat{f}(1,z) = 2r - 1 \tag{3.1}$$

while, from $\sum_{\ell=1}^{\ell_{\max}} h_\ell = r_{\ell_{\max}+1} r_{\ell_{\max}}$, we get

$$\hat{h}(1,z) = r^2. \tag{3.2}$$

From (2.35) and (2.39), this leads to

$$\hat{e}(1,z) = 2\frac{r-1}{r^2} = 2zr = \sum_{n\geqslant 1} \frac{2(3n-3)!}{(2n-1)!(n-1)!} z^n$$

$$\hat{g}(1,z) = 1 - \frac{1}{r^2} = zr(r+1) = \sum_{n\geqslant 1} \frac{2(3n-3)!}{(2n-2)!n!} z^n. \tag{3.3}$$

These expressions are consistent with (2.15) as they give

$$\frac{\hat{e}(1,z)|_{z^n}}{p_1|_{z^n}} = n$$

$$\frac{\hat{g}(1,z)|_{z^n}}{p_1|_{z^n}} = 2n-1 \tag{3.4}$$

where we recognize the number $n = (n+2) - 2$ of vertices different from the two extremities of the root edge in a rooted quadrangulation and the number $(2n-1)$ of edges different from the root edge. This is expected since in $\hat{e}(1,z)$ (respectively $\hat{g}(1,z)$), there is no condition of distance for the marked vertex (respectively the second marked edge).

Finally, from (2.42), we also have

$$\frac{\hat{p}(1,z)|_{z^n}}{p_1|_{z^n}} = 1 + \frac{n}{2} = \frac{n+2}{2} \tag{3.5}$$

consistent with the fact that $\hat{p}(1,z)$ and p_1 both count maps with a marked edge, with an extra origin vertex in $\hat{p}(1,z)$ ($n+2$ choices) and an extra orientation for the marked edge in p_1 (2 choices).

From the explicit forms (2.28) and (2.29) of f_ℓ and h_ℓ, and via relations (2.33), (2.37) and (2.40) (or their compact forms (2.35), (2.39) and (2.42)), we have an implicit access to the desired functions e_ℓ, g_ℓ and p_ℓ. Explicit expressions may easily be obtained for the first values of ℓ. Taking $\ell = 1, 2, 3$, we deduce for instance the first terms in the z expansion of p_ℓ, g_ℓ and e_ℓ:

$$\begin{aligned}
p_1(z) &= 2z + z^2 + 2z^3 + 6z^4 + 22z^5 + 91z^6 + 408z^7 + 1938z^8 + 9614z^9 + \cdots \\
p_2(z) &= g_1(z) = e_1(z) \\
&= z + z^2 + 3z^3 + 11z^4 + 46z^5 + 209z^6 + 1006z^7 + 5053z^8 + 26\,227z^9 + \cdots \\
g_2(z) &= z + 2z^2 + 7z^3 + 29z^4 + 132z^5 + 639z^6 + 3232z^7 + 16\,896z^8 + 90\,643z^9 + \cdots \\
e_2(z) &= z + z^2 + 3z^3 + 12z^4 + 55z^5 + 272z^6 + 1411z^7 + 7565z^8 + 41\,560z^9 + \cdots \\
p_3(z) &= z^4 + 9z^5 + 63z^6 + 405z^7 + 2512z^8 + 15\,333z^9 + \cdots \\
g_3(z) &= 2z^4 + 20z^5 + 151z^6 + 1030z^7 + 6705z^8 + 42\,617z^9 + \cdots \\
e_3(z) &= z^4 + 9z^5 + 64z^6 + 422z^7 + 2698z^8 + 17\,011z^9 + \cdots .
\end{aligned} \tag{3.6}$$

More explicit distance-dependent results may be extracted from the above implicit form of e_ℓ, g_ℓ or p_ℓ *in the limit of large quadrangulations*, i.e. when $n \to \infty$. This can be done by keeping ℓ finite, giving rise to the so-called local limit, or by letting ℓ scale as $n^{1/4}$, leading to the so-called scaling limit. Let us now discuss these two cases in detail.

3.2. Local limit laws for large quadrangulations with no multiple edges

The large n asymptotics of quadrangulations with no multiple edges may be extracted from the singular behavior of the various generating functions above when z approaches its critical value equal to $4/27$ as apparent for instance in (2.13). Writing

$$z = \frac{4}{27}(1 - \eta^2) \tag{3.7}$$

we have for instance the small η expansion

$$p_1 = \frac{1}{3} - \frac{4}{9}\eta^2 + \frac{8}{27\sqrt{3}}\eta^3 + \cdots \tag{3.8}$$

with no term proportional to η, so that the leading singular part of p_1 is coded by the coefficient of η^3. We immediately deduce the large n behavior

$$p_1|_{z^n} \sim \left(\frac{27}{4}\right)^n \frac{8}{27\sqrt{3}n^{5/2}} \frac{1}{\Gamma(-3/2)} = \left(\frac{27}{4}\right)^n \frac{2}{9\sqrt{3\pi}n^{5/2}} \tag{3.9}$$

a result which can alternatively be obtained from the explicit expression of $p_1|_{z^n}$ read off (2.15). Similarly, we get from the explicit forms (2.28) and (2.29) of f_ℓ and h_ℓ small η expansions for $\hat{f}(t, z)$ and $\hat{h}(t, z)$ of the form

$$\begin{aligned}
\hat{f}(t, z) &= \hat{A}^{(f)}(t) + \hat{C}^{(f)}(t)\eta^2 + \hat{D}^{(f)}(t)\eta^3 + \cdots \\
\hat{h}(t, z) &= \hat{A}^{(h)}(t) + \hat{C}^{(h)}(t)\eta^2 + \hat{D}^{(h)}(t)\eta^3 + \cdots
\end{aligned} \tag{3.10}$$

with coefficients which can be computed explicitly, and with again a leading singular behavior coded by the coefficient of η^3. We deduce from (2.33) and (2.37) the expansions

$$\begin{aligned}
\hat{e}(t, z) &= \hat{A}^{(e)}(t) + \hat{C}^{(e)}(t)\eta^2 + \hat{D}^{(e)}(t)\eta^3 + \cdots \\
\hat{g}(t, z) &= \hat{A}^{(g)}(t) + \hat{C}^{(g)}(t)\eta^2 + \hat{D}^{(g)}(t)\eta^3 + \cdots
\end{aligned} \tag{3.11}$$

where, in particular,

$$\hat{D}^{(e)}(t) = \frac{\hat{D}^{(h)}(t) - \hat{A}^{(f)}(t)\hat{D}^{(h)}(t) + \hat{A}^{(h)}(t)\hat{D}^{(f)}(t)}{(\hat{A}^{(h)}(t))^2}$$

$$\hat{D}^{(g)}(t) = \frac{\hat{D}^{(h)}(t)}{(\hat{A}^{(h)}(t))^2}. \tag{3.12}$$

Doing the explicit computation for these two quantities, we find

$$\begin{aligned}\hat{D}^{(e)}(t) = {} & \frac{4(t+1)}{945\sqrt{3}t(1-t)^4(t(3t-4)+4(1-t)\mathrm{Li}_2(t))^2} \\ & \times \{t(12(1-t)^2\log(1-t)(9t^5-13t^4-49t^3+128t^2-57t+12) \\ & + t(-175t^6+554t^5+89t^4-2292t^3+2610t^2-900t+144)) - 12(1-t)\mathrm{Li}_2(t) \\ & \times (12(1-t)^6\log(1-t) + t(8t^6-33t^5+64t^4-103t^3+148t^2-66t+12))\} \\ \hat{D}^{(g)}(t) = {} & \frac{16t^3(t(35t^4-151t^3+236t^2-114t+24) - 24(1-t)^5\mathrm{Li}_2(t))}{945\sqrt{3}(1-t)^4(t(3t-4)+4(1-t)\mathrm{Li}_2(t))^2}\end{aligned} \tag{3.13}$$

where $\mathrm{Li}_2(t) = \sum_{k\geqslant 1}\frac{t^k}{k^2}$. These functions encode the average number $\langle V_\ell\rangle$ of vertices at distance ℓ (respectively $\langle E_\ell\rangle$ of edges of type $(\ell-1)\to\ell$) in rooted quadrangulations with no multiple edges in the limit of large size n. Indeed, we have

$$\langle V_\ell\rangle = \delta_{\ell,1} + \lim_{n\to\infty}\frac{e_\ell|_{z^n}}{p_1|_{z^n}} = \delta_{\ell,1} + \frac{27\sqrt{3}}{8}\hat{D}^{(e)}|_{t^{\ell-1}}$$

$$\langle E_\ell\rangle = \delta_{\ell,1} + \lim_{n\to\infty}\frac{h_\ell|_{z^n}}{p_1|_{z^n}} = \delta_{\ell,1} + \frac{27\sqrt{3}}{8}\hat{D}^{(g)}|_{t^{\ell-1}} \tag{3.14}$$

or equivalently

$$\sum_{\ell\geqslant 0} t^\ell\langle V_{\ell+1}\rangle = 1 + \frac{27\sqrt{3}}{8}\hat{D}^{(e)}(t)$$

$$\sum_{\ell\geqslant 0} t^\ell\langle E_{\ell+1}\rangle = 1 + \frac{27\sqrt{3}}{8}\hat{D}^{(g)}(t). \tag{3.15}$$

Expanding $\hat{D}^{(e)}(t)$ and $\hat{D}^{(g)}(t)$ at small t, we get for instance

$$\begin{aligned}&\langle V_1\rangle = \tfrac{133}{25}, \qquad \langle V_2\rangle = \tfrac{1809}{125}, \qquad \langle V_3\rangle = \tfrac{90\,747}{3125} \\ &\langle E_1\rangle = \tfrac{133}{25}, \qquad \langle E_2\rangle = \tfrac{2727}{125}, \qquad \langle E_3\rangle = \tfrac{598\,563}{12\,500}.\end{aligned} \tag{3.16}$$

For $t\to 1$, we have

$$\hat{D}^{(e)}(t) \sim \frac{16}{63\sqrt{3}}\frac{1}{(1-t)^4}, \qquad \hat{D}^{(g)}(t) \sim \frac{32}{63\sqrt{3}}\frac{1}{(1-t)^4} \tag{3.17}$$

from which we deduce the large ℓ behaviors

$$\langle V_\ell\rangle \sim \tfrac{1}{7}\ell^3, \qquad \langle E_\ell\rangle \sim \tfrac{2}{7}\ell^3. \tag{3.18}$$

We may finally extract from the expansion of $\hat{p}(t,z)$ the average number $\langle E_\ell\rangle_\bullet$ of edges at distance ℓ from the origin now in the ensemble of pointed quadrangulations of fixed large size n. We find

$$\langle E_1\rangle_\bullet = 4, \qquad \langle E_2\rangle_\bullet = \tfrac{432}{25}, \qquad \langle E_3\rangle_\bullet = \tfrac{5076}{125}, \tag{3.19}$$

i.e. the statistics of neighbors are slightly different in rooted and pointed quadrangulations, as expected. Still, for large ℓ, we get

$$\langle E_\ell\rangle_\bullet \sim \tfrac{2}{7}\ell^3 \tag{3.20}$$

and pointed and rooted maps give rise to the same statistics in this limit.

3.3. Scaling limit laws for large quadrangulations with no multiple edges

A non-trivial scaling limit is obtained by letting z tend to its critical value $4/27$ and letting ℓ become large as

$$z = \tfrac{4}{27}(1-\eta^2), \qquad \ell = L\eta^{-1/2} \tag{3.21}$$

with $\eta \to 0$ and L finite. Using the small η behavior $y \sim \mathrm{e}^{-2\alpha\,\eta^{1/2}}$ with $\alpha = 3^{1/4}/\sqrt{2}$, we find the leading behavior

$$h_\ell \sim -\tfrac{9}{2}\eta^{3/2}\,\mathcal{F}'(L;3^{1/4}/\sqrt{2}) \tag{3.22}$$

where we introduce the scaling function

$$\mathcal{F}(L;\alpha) = \frac{2\alpha^2}{3}\left(1+\frac{3}{\sinh(\alpha L)^2}\right) \tag{3.23}$$

and where $\mathcal{F}'$ stands for the derivative of $\mathcal{F}$ with respect to L. We recognize here the scaling function $\mathcal{F}$ encountered [13] when computing the scaling limit of the two-point function in the context of general (with possibly multiple edges) quadrangulations. Note that the value of α in this latter case is however different, equal to $\sqrt{3/2}$. This is not a surprise since, from the substitution approach, the vicinity of the critical point $z = 4/27$ corresponds precisely to the vicinity of the critical point $g = 1/12$ for general quadrangulations. From (2.19), we indeed have the expansion

$$g\left(\tfrac{4}{27}(1-\eta^2)\right) = \tfrac{1}{12}\left(1-\tfrac{1}{3}\eta^2+\mathcal{O}(\eta^3)\right) \tag{3.24}$$

so that expanding in $\sqrt{1-27z/4}$ amounts to expanding in $\sqrt{3}\,\sqrt{1-12g}$ and the change of normalization by $\sqrt{3}$ simply translates into a change of the value of α by $3^{1/4}$.

Rather than that of h_ℓ, let us now explore the scaling form of g_ℓ itself, which is relevant to the statistics of distances in quadrangulations with no multiple edges. This requires a few manipulations as follows. Right at the critical value $z = 4/27$, we have

$$h_\ell(4/27) = 9\frac{(2\ell+3)}{(\ell+1)^2(\ell+2)^2} \tag{3.25}$$

so that, in the scaling limit (3.21), we may write at leading order in η

$$h_\ell(z) - h_\ell(4/27) \sim \eta^{3/2}\left(-\frac{9}{2}\,\mathcal{F}'(L;3^{1/4}/\sqrt{2}) - \frac{18}{L^3}\right). \tag{3.26}$$

Setting

$$t = 1 - s\eta^{1/2} \tag{3.27}$$

this translates into

$$\hat{h}(t,z) - \hat{h}(t,4/27) \sim \eta \int_0^\infty \mathrm{d}L\,\mathrm{e}^{-sL}\left(-\frac{9}{2}\,\mathcal{F}'(L;3^{1/4}/\sqrt{2}) - \frac{18}{L^3}\right) \tag{3.28}$$

with, from (3.25),

$$\begin{aligned}\hat{h}(t,4/27) &= -\frac{9(t(3t-4)+4(1-t)\mathrm{Li}_2(t))}{4t^3}\\ &= \frac{9}{4}+\frac{3}{4}(15-2\pi^2)s\eta^{1/2} - \frac{9}{4}(s^2\eta(4\log(s\eta^{1/2})+2\pi^2-13)) + \mathcal{O}(\eta^{3/2}).\end{aligned} \tag{3.29}$$

From (2.35), this leads to

$$\hat{g}(t,z) - \hat{g}(t,4/27) \sim \frac{16}{81}\,\eta \int_0^\infty \mathrm{d}L\,\mathrm{e}^{-sL}\left(-\frac{9}{2}\,\mathcal{F}'(L;3^{1/4}/\sqrt{2}) - \frac{18}{L^3}\right) \tag{3.30}$$

with

$$\hat{g}(t,4/27) = 1 - \frac{1}{\hat{h}(t,4/27)}$$
$$= \frac{5}{9} + \frac{4}{27}(15 - 2\pi^2)s\eta^{1/2} - \frac{8}{81}(s^2\eta(18\log(s\eta^{1/2}) + 2\pi^4 - 21\pi^2 + 54)) + \mathcal{O}(\eta^{3/2}). \tag{3.31}$$

From the singular part of $\hat{g}(t,4/27)$ when $t \to 1$ (i.e. $s \to 0$), we deduce the large ℓ behavior

$$g_\ell(4/27) \sim \frac{32}{9\ell^3} = \eta^{3/2}\frac{32}{9L^3} \tag{3.32}$$

and from (3.30), we deduce eventually

$$g_\ell - g_\ell(4/27) \sim \eta^{3/2}\left(-\frac{8}{9}\,\mathcal{F}'(L;3^{1/4}/\sqrt{2}) - \frac{32}{9L^3}\right)$$
$$\text{i.e.} \quad g_\ell \sim -\frac{8}{9}\eta^{3/2}\mathcal{F}'(L;3^{1/4}/\sqrt{2}). \tag{3.33}$$

The net result of passing from h_ℓ to g_ℓ is therefore a simple normalization factor (8/9 for g_ℓ instead of 9/2 for h_ℓ). This factor is important as it will ensure a proper normalization of the two-point function but g_ℓ behaves essentially as h_ℓ which, from the substitution approach, is characterized by the same scaling function as for general quadrangulations, up to a change of scale by $3^{1/4}$.

Now the above result may be used to study the two-point distance statistics in the ensemble of quadrangulations with no multiple edges having a fixed size n (= number of faces), in the limit of large n . As explained in [13], the term of order z^n in the various generating functions above may be extracted by a contour integral in z which at large n translates via a saddle point estimate into an integral over a real variable ζ upon setting

$$z = \frac{4}{27}\left(1 + \frac{\zeta^2}{n}\right). \tag{3.34}$$

Setting now

$$\ell = rn^{1/4} \tag{3.35}$$

we may use the above formulas with $\eta = -\mathrm{i}\zeta\, n^{-1/2}$ and $L = \sqrt{-\mathrm{i}\zeta}\, r$ to deduce the probability $\tilde{\rho}(r)$ that a marked edge picked uniformly at random in a rooted quadrangulation with no multiple edges be at rescaled distance r from the root edge:

$$\tilde{\rho}(r) = \lim_{n\to\infty} n^{1/4}\,\frac{1}{2n}\,\frac{g_\ell|_{z^n}}{p_1|_{z^n}}$$
$$= \lim_{n\to\infty} n^{1/4}\frac{1}{2n}\frac{9\sqrt{3\pi}}{2}n^{5/2}\frac{1}{\pi n}\int_{-\infty}^{\infty}\mathrm{d}\zeta(-\mathrm{i}\zeta)\mathrm{e}^{-\zeta^2}\left(\frac{-\mathrm{i}\zeta}{n^{1/2}}\right)^{3/2}\left(-\frac{8}{9}\right)\mathcal{F}'(\sqrt{-\mathrm{i}\zeta}\; r;3^{1/4}/\sqrt{2})$$
$$= \frac{2\sqrt{3}}{\sqrt{\pi}}\int_{-\infty}^{\infty}\mathrm{d}\zeta\,\mathrm{i}\zeta\;\mathrm{e}^{-\zeta^2}\mathcal{F}'(r;3^{1/4}/\sqrt{2}\sqrt{-\mathrm{i}\zeta}) \tag{3.36}$$

where we used the self-similarity property $\mathcal{F}'(u\,r;\alpha) = u^{-3}\mathcal{F}'(r;\alpha\,u)$.

We could repeat all the above calculations for e_ℓ instead of g_ℓ. This leads to the same scaling form $\tilde{\rho}(r)$ for the probability that a marked vertex picked uniformly at random in a rooted quadrangulation with no multiple edges be at rescaled distance r from the root edge. This is expected as vertices cannot be distinguished from edges in the scaling limit. We could also use p_ℓ and again, we would get the same scaling form for the probability that a marked

edge picked uniformly at random in a pointed quadrangulation with no multiple edges be at rescaled distance r from the root origin vertex.

We may now compare the above result with the density of points (vertices or edges) at distance $\ell = rn^{1/4}$ in general quadrangulations of size n, in the limit $n \to \infty$. It is given by [13]

$$\rho(r) = \frac{2}{\sqrt{\pi}} \int_{-\infty}^{\infty} \mathrm{d}\zeta \, \mathrm{i}\zeta \; \mathrm{e}^{-\zeta^2} \mathcal{F}'(r; \sqrt{3/2}\sqrt{-\mathrm{i}\zeta}) \tag{3.37}$$

so that, using again the self-similarity of $\mathcal{F}'$, we may write

$$\tilde{\rho}(r) = \frac{1}{3^{1/4}} \rho\left(\frac{r}{3^{1/4}}\right). \tag{3.38}$$

This may be viewed as a manifestation of the universal nature of the two-point function, which is the same for the two classes (with or without multiple edges) of maps, up to some global (non-universal) scale. In the present case, this universality can simply be traced back in the calculations and comes from the fact that passing from H_ℓ to h_ℓ is a simple substitution $g \leftrightarrow z$ (which explains the factor $3^{1/4}$) and then passing from h_ℓ to g_ℓ simply amounts to some global normalization.

Since the rescaled distance is obtained by normalizing the original distance by $n^{1/4}$, the rescaling factor above states that general quadrangulations with size n are asymptotically isometric to quadrangulations with no multiple edges of size $(n/3)$. This result is consistent with the heuristic picture of a general quadrangulation as made of a large component, the *'mother universe'*, with no multiple edges and of typical size $n/3$, and of small components, the *'baby universes'*, of finite extension. The two-point function of general quadrangulations is entirely dictated by the distance statistics in their mother universes. This is because the parts of geodesics lying in baby universes are of negligible length.

4. Mother universe and minbus in general quadrangulations

In this section, we return to the case of general quadrangulations and discuss their geometry in the light of our new results. As just explained, the geometry of the mother universe itself is well captured by the two-point function. In contrast, this two point-function is blind to the geometry of minimal neck baby universes. Here we compute a number of distance-dependent quantities characterizing the minbus. To this end, let us first discuss how our various generating functions for almost well-balanced trees translate into the language of general quadrangulations. Their meaning is best captured by reformulating the substitution of section 2.3 directly *at the level of the maps*.

4.1. Substitution for rooted maps

Out of any *rooted* general quadrangulation, we may extract a quadrangulation with no multiple edges as follows. Consider two fixed vertices adjacent in the quadrangulation and connected by exactly k edges ($k \geqslant 1$), which we may orient for convenience from the vertex closest to the origin of the root edge to the other vertex. These edges separate the map into k *elementary domains* and the *root face* of the map, i.e. the face immediately on the left of the root edge, belongs to exactly one of them. Let us consider the 'outgrowth' formed by the union of the $(k-1)$ elementary domains not containing the root face. This outgrowth is either empty (if $k = 1$) or it is a quadrangulation with a boundary of length 2 which, upon continuous deformation in the sphere, may be glued into a single oriented edge. The outgrowth may therefore be described as a (possibly empty) rooted quadrangulation itself.

Moreover, if we now consider all pairs of vertices linked by more than one edge, and the corresponding (non-empty) outgrowths, the interiors of these outgrowths form a forest (i.e. any two of them are either disjoint or included one into the other), which allows us to select *maximal outgrowth* (i.e. those not contained in a bigger one). If we now squeeze into a single edge each of these maximal outgrowths, we end up with a quadrangulation with no multiple edges which is naturally rooted at the original root edge. Conversely, a general rooted quadrangulation is obtained from a quadrangulation with no multiple edges by inflating each edge into an outgrowth as above. If we assign a weight g per face of the general quadrangulation, the generating function describing a squeezed outgrowth is that, $R_1(g)$, of rooted quadrangulations (including a first term 1 in R_1 for the empty case). This results in the identity

$$R_1(g) = 1 + p_1(g(R_1(g))^2) \tag{4.1}$$

relating the generating function R_1 of rooted general quadrangulations to that p_1 of rooted quadrangulations with no multiple edges. In (4.1), we used the fact that there are twice as many edges as faces in a quadrangulation, so assigning a weight g per face and a weight $R_1(g)$ per edge is equivalent to assigning a weight $z = g\ (R_1(g))^2$ per face only. Introducing $z(g)$ as in (2.19), and its inverse $g(z)$, equation (4.1) reads $p_1(z) = R_1(g(z)) - 1$. Using $R_1 = R - gR^3 = (1 + 3gR^2)(1 - gR^2)$ at $g = g(z)$ (where $gR^2 = zr^2$), we recover $p_1 = (1 + 3zr^2)(1 - zr^2) - 1 = zr(3 - r)$ as expected. The above construction allows us to define for each rooted quadrangulation its *core*, which is the rooted quadrangulations with no multiple edges obtained after the squeezing procedure.

The above connection was studied in detail in [15] in the slightly different, but equivalent context of general and 2-connected maps. Translated into our language, the result is that, in the ensemble of rooted quadrangulations with a fixed size n, and in the limit $n \to \infty$, the law for the size (number of faces) of the core is bimodal: with probability $2/3$, the core remains finite while, with probability $1/3$, it is macroscopic, of size $n/3 + \alpha n^{2/3}$ with α distributed according to a *standard Airy distribution*. Rather than focusing on the core itself, which depends strongly on the choice of root edge, one may fully decompose the rooted quadrangulation into components with no multiple edges by applying recursively the squeezing procedure inside each of the squeezed outgrowths (which may themselves be viewed as rooted quadrangulations as explained above). Alternatively, this procedure amounts to disconnecting the map into pieces by cutting along all its minimal necks, which are the cycles of length 2 in the map and then gluing the necks into single edges. Each of the obtained component is a rooted quadrangulation with no multiple edges. In the limit of large n, the largest component has size $n/3 + \alpha n^{2/3}$ as above while the second largest one has size at most $n^{2/3}$. Adopting the terminology of quantum gravity, the largest component defines precisely the mother universe, while the other components, once reglued together, form the minimal neck baby universes (minbus). A detailed heuristic discussion of minbus can be found in [16]. In particular, it is shown that, in all generality, the largest minbu has a size of order $n^{1/(1-\gamma_{\text{string}})}$ where γ_{string} is the so-called string susceptibility exponent, equal to $-1/2$ for pure gravity.

4.2. Substitution for maps with two marked points

The above squeezing procedure dealt with quadrangulations with a marked root edge only, as counted by R_1. We now wish to apply a similar squeezing procedure to the configurations with two marked points (edge or vertex) distant by ℓ. More precisely, let us start with general rooted quadrangulations with an extra marked vertex at distance ℓ from the origin of the root edge, as counted by F_ℓ. Let us suppose first that $\ell > 1$ so that, in particular, the marked

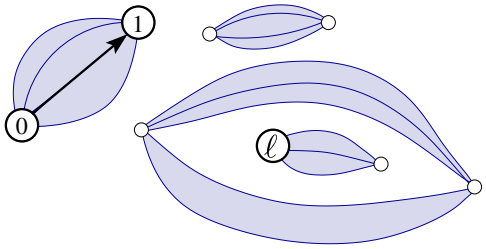

Figure 6. The squeezing procedure for a rooted map with a marked vertex at distance ℓ (distinct from the endpoint of the root edge if $\ell = 1$). If the root edge itself is a multiple edge, we squeeze all the associated elementary domains (filled regions) except that containing the marked vertex. For any other pair of vertices linked by multiple edges, we squeeze the associated elementary domains (filled regions) except that containing the root edge and that containing (strictly) the marked vertex. These two unsqueezed domains may be the same or not. In practice, it is sufficient to squeeze the maximal domains only.

vertex is different from the endpoint of the root edge. If the extremities of the root edge are linked by $k > 1$ edges, delimiting k elementary domains, we start by squeezing into a single oriented edge the outgrowth formed by the union of the $(k-1)$ such elementary domains not containing the marked vertex (see figure 6 for an illustration). This oriented edge becomes the new root edge. Note that the choice of outgrowth here is slightly different from that adopted above for rooted quadrangulations without a marked vertex. In particular the outgrowth is now formed in general of two pieces, one on each side of the original root edge, and separated on the sphere by the marked vertex. Its contribution to F_ℓ is thus counted by $(R_1(g))^2$. For any other pair of vertices, we look at the outgrowth formed by the union of all the associated elementary domains except that containing the root edge and, if the marked vertex is not one of the two vertices in the pair, that containing the marked vertex. Note that this second excluded elementary domain may be the same as the first one or not, so that the outgrowth consists either of one connected piece or of two pieces separating the root edge from the marked vertex (see figure 6). Considering all pairs of vertices linked by more than one edge, the interior of the corresponding (non-empty) outgrowths forms again a forest among which we select the maximal outgrowths that we squeeze into single edges. After squeezing, we end up with a rooted quadrangulation with an extra marked vertex at distance ℓ from the origin of the root edge, and satisfying

(1) all edges are simple or double edges;
(2) the root edge is a simple edge;
(3) a double edge necessarily separates strictly the root edge from the marked vertex.

The fact that the marked vertex is still at distance ℓ from the origin of the root edge is because the original geodesic paths never enter strictly the outgrowths which have been squeezed, so these paths are still present in the squeezed object and no shorter path has been created. If we denote by $f_\ell(z)$ the generating function for such quadrangulations with a weight z per face, the above substitution procedure translates into the relation

$$F_\ell(g) = R_1(g)\ f_\ell(g(R_1(g))^2) \tag{4.2}$$

since each edge of the quadrangulations counted by f_ℓ has to be substituted by an outgrowth (counted by $R_1(g)$), except for the root edge whose outgrowth is counted by $(R_1(g))^2$, hence the extra multiplicative factor $R_1(g)$. The above relation precisely matches (2.30), so our new definition of f_ℓ matches its former definition of section 2.4 in terms of chains of trees. In other

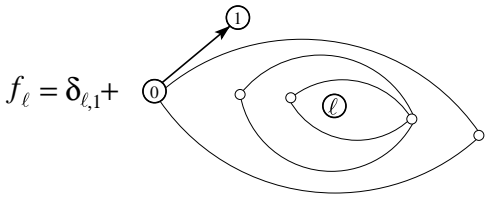

Figure 7. The generating function f_ℓ enumerates rooted quadrangulations with a marked vertex at distance ℓ from the origin of the root edge (and different from its endpoint if $\ell = 1$), with only single and double edges. The root edge is necessarily a single edge and double edges necessarily separate (strictly) the marked vertex from the root edge. For $\ell = 1$, a term 1 is added to f_ℓ to guarantee relation (4.2) or equivalently (2.30).

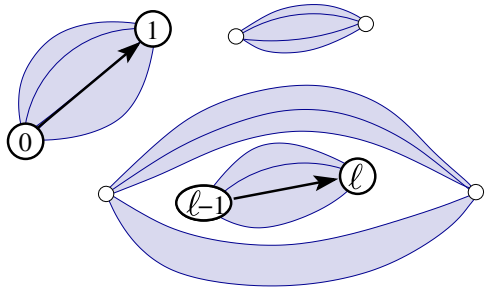

Figure 8. The squeezing procedure for a rooted map with a marked edge of type $(\ell-1) \to \ell$ with respect to the origin of the root edge (and whose endpoint is distinct from the endpoint of the root edge if $\ell = 1$). If the root edge itself is a multiple edge, we squeeze all the associated elementary domains (filled regions) except that containing the marked vertex. Similarly, if the marked edge is a multiple edge, we squeeze all the associated elementary domains (filled regions) except that containing the root edge. For any other pair of vertices linked by multiple edges, we squeeze the associated elementary domains (filled regions) except that containing the root edge and that containing the marked edge. These two unsqueezed domains may be the same or not. In practice, it is sufficient to squeeze the maximal domains.

words, we end up with a direct interpretation of the quantity f_ℓ of section 2.4 as counting rooted quadrangulations with a marked vertex at distance ℓ, and satisfying (1)–(3) above.

If $\ell = 1$, i.e. if we start with a rooted quadrangulation with an extra marked vertex at distance 1 from the origin, we may apply exactly the same squeezing procedure provided that the marked vertex be different from the endpoint of the root edge. If the marked vertex happens to be the endpoint of the root edge, we decide to squeeze all the associated elementary domains, resulting into a trivial object made of the root edge itself. This procedure ensures that equation (4.2) above holds for $\ell = 1$: $f_1(z)$ contains a constant term 1 accounting for the trivial case above while $f_1(z) - 1$ is the generating function for rooted quadrangulations with an extra marked vertex adjacent to the origin but non-incident to the root, and satisfying (1)–(3) above. The interpretation of f_ℓ for $\ell \geqslant 1$ is illustrated in figure 7.

As for H_ℓ, recall that it counts rooted general quadrangulations with an extra marked edge of type $(\ell - 1) \to \ell$ with respect to the origin of the root edge. Assuming again that $\ell > 1$ so that this marked edge has an endpoint different from that of the root edge, we squeeze the outgrowths on both sides of the root edge and on both sides of the marked edge, transforming these edges into single edges (see figure 8). Repeating the above arguments, we see that, upon squeezing of the maximal outgrowth not containing the two marked edges, H_ℓ is related via

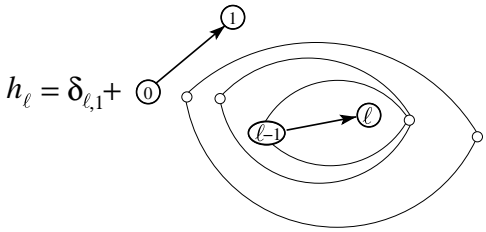

Figure 9. The generating function h_ℓ enumerates rooted quadrangulations with a marked edge of type $(\ell-1) \to \ell$ with respect to the origin of the root edge (and with its endpoint different from the endpoint of the root edge if $\ell = 1$), with only single and double edges. The root edge and the marked edge are necessarily single edges and double edges necessarily separate the marked edge from the root edge. For $\ell = 1$, a term 1 is added to h_ℓ to guarantee relation (2.30).

(2.30) to the generating function $h_\ell(z)$ for rooted quadrangulations with an extra marked edge of type $(\ell-1) \to \ell$ with respect to the origin of the root edge, and satisfying

(1)′ all edges are simple or double edges;
(2)′ the root edge and the extra marked edge are simple edges;
(3)′ a double edge necessarily separates strictly the root edge from the extra marked edge.

Again when $\ell = 1$, equation (2.30) still holds with h_1 composed of a trivial constant term 1 (accounting for the case where the root edge and the extra marked edge have the same endpoint in the configuration counted by H_1) and of the generating function $h_1 - 1$ of rooted quadrangulations with an extra marked edge incident to the origin of the root edge but with a different endpoint, and satisfying (1)′–(3)′. This interpretation of h_ℓ is illustrated in figure 9.

We may now easily understand relations (2.31) and (2.36) directly in the language of quadrangulations. From (3) or (3)′, the double edges in f_ℓ or h_ℓ are necessarily *nested* and of type $(k-1) \to k$ for increasing (non-necessarily consecutive) values of k in the range $[1, \ell]$, if we sort them from the root edge to the marked vertex (respectively edge) at distance ℓ. Moreover, the marked vertex (respectively the endpoint of the marked edge) at distance ℓ from the origin of the map is at distance $\ell + 1 - k$ of the first extremity (i.e. the vertex at distance $k-1$ from the origin of the map) of any double edge of type $(k-1) \to k$. This is because any geodesic path from the origin to the marked vertex (respectively endpoint) must pass through one of the extremities of the double edge and we can always find one geodesic passing through the first extremity with label $(k-1)$.

Starting now from a configuration counted by f_ℓ (respectively h_ℓ), if it contains no double edge, it is then a configuration counted by e_ℓ (respectively g_ℓ). Otherwise, looking at the double edge closest to the root edge, i.e. corresponding to the smallest value of k above, this double edge separates the map into two domains: one containing the root edge and the other the marked vertex (respectively edge) at distance ℓ. Upon squeezing this latter domain into a simple edge of type $(k-1) \to k$, we end up with a rooted quadrangulation with no multiple edges and with a marked edge of type $(k-1) \to k$, hence counted by g_k. The squeezed domain is a quadrangulation with a boundary of length 2 which, upon continuous deformation in the sphere, can be glued into a single oriented edge which defines a new root edge. This gives rise again to a rooted quadrangulation with now a marked vertex (respectively edge) at distance $(\ell + 1 - k)$ (respectively of type $(\ell - k) \to (\ell + 1 - k)$) with respect to the origin of the new root edge. The squeezed domain satisfies conditions (1)–(3) (respectively (1)′–(3)′) and the corresponding generating function is therefore $f_{\ell+1-k}$ (respectively $h_{\ell+1-k}$) for $k < \ell$

and $(f_1 - 1)$ (respectively $h_1 - 1$) if $k = \ell$. This leads to the desired relations (2.36) and (2.31) for $\ell > 1$. As before the case $\ell = 1$ requires more care but it is easily seen to reproduce the relations of the previous section.

Finally, from $f_\ell = r_{\ell+1} - r_{\ell-1} = q_\ell + q_{\ell+1}$, we have, via a simple re-rooting, an interpretation of q_ℓ for $\ell > 1$ as counting pointed quadrangulations with a marked edge of type $(\ell - 1) \to \ell$ satisfying

(1)$''$ all edges are simple or double edges;
(2)$''$ the marked edge is a simple edge;
(3)$''$ a double edge necessarily separates strictly the origin from the marked edge.

4.3. Geometry of minbus

We may use the above interpretation of our generating functions to explore the geometry of minbus. We consider in this section the ensemble of *bi-rooted* quadrangulations where the two marked edges are at distance ℓ, as enumerated by H_ℓ. For any configuration in this ensemble, the squeezing procedure in section 4.2 produces a *bi-rooted* configuration with again its two marked edges at distance ℓ, and satisfying (1)$'$–(3)$'$ above. We shall call this configuration the *kernel* of the bi-rooted quadrangulation. Note that this is a notion slightly different from the core as it involves two marked edges rather than one. In particular, the kernel may now contain double edges which correspond to minimal necks encountered along any geodesic path linking the origins of the two marked edges. If we decompose as before the quadrangulation into components with no multiple edge, the kernel may then be viewed as a linear sequence of such components glued via minimal necks. We may now condition the size of the original quadrangulation to be n and compute the probability that its kernel has size (= number of faces) k. It simply reads

$$\mathcal{P}_\ell^{(n)}(k) = \frac{h_\ell|_{z^k} \times R_1^2 \left(g R_1^2\right)^k\big|_{g^n}}{H_\ell|_{g^n}} \tag{4.3}$$

and, at large n, the leading behavior of the g^n coefficients may be extracted by a simple singularity analysis. Setting $g = \frac{1}{12}(1 - \epsilon^2)$, we have

$$H_\ell = A_\ell + C_\ell \epsilon^2 + D_\ell \epsilon^3 + \cdots$$
$$\text{with} \qquad D_\ell = \frac{8\ell(\ell+3)(2\ell+3)(5\ell^4 + 30\ell^3 + 67\ell^2 + 66\ell + 28)}{35(\ell+1)^2(\ell+2)^2} \tag{4.4}$$

while

$$R_1^2 \left(g R_1^2\right)^k = \frac{16}{9}\left(\frac{4}{27}\right)^k (1 - (2+3k)\epsilon^2 + 4(1+k)\epsilon^3 + \cdots). \tag{4.5}$$

Picking the singular ($\propto \epsilon^3$) term, we get when $n \to \infty$

$$\mathcal{P}_\ell^{(\infty)}(k) = \frac{64}{9 D_\ell} h_\ell|_{z^k} (1+k) \left(\frac{4}{27}\right)^k. \tag{4.6}$$

For $\ell = 1$, which corresponds to two marked edges having the same origin, we have in particular a probability $\mathcal{P}_1^{(\infty)}(0) = 2/7$ that the kernel be empty, which happens when the marked edges also have the same endpoint. More interestingly, if we sum $\mathcal{P}_\ell^{(\infty)}(k)$ over all (finite) values of k, we get the probability that the kernel remains finite:

$$\sum_{k=0}^{\infty} \mathcal{P}_\ell^{(\infty)}(k) = \frac{64}{9 D_\ell}\left(h_\ell\left(\frac{4}{27}\right) + \frac{4}{27} h'_\ell\left(\frac{4}{27}\right)\right)$$
$$= \frac{14(\ell^2 + 3\ell + 4)}{5\ell^4 + 30\ell^3 + 67\ell^2 + 66\ell + 28} \overset{\ell \gg 1}{\sim} \frac{14}{5\ell^2}. \tag{4.7}$$

This is the probability that the kernel does not include the mother universe as one of its components, i.e. the probability that we may go from one edge to the other without entering the mother universe. In other words, this is nothing but the *probability that the two marked edges lie in the same baby universe*. This probability tends to 0 at large ℓ like $1/\ell^2$.

By a slight change of normalization in the above calculation, we may return to the ensemble of rooted quadrangulations of size n and compute the *average number* of edges lying at distance ℓ from the root edge and defining with this root edge a kernel of size k. This number is given by

$$\mathcal{N}_\ell^{(n)}(k) = \frac{h_\ell|_{z^k} \times R_1^2 \left(g R_1^2\right)^k \Big|_{g^n}}{R_1|_{g^n}} \overset{n\to\infty}{\sim} \frac{8}{3} h_\ell|_{z^k}(1+k)\left(\frac{4}{27}\right)^k. \tag{4.8}$$

Upon summing over all (finite) values of k, we get

$$\sum_{k=0}^{\infty} \mathcal{N}_\ell^{(\infty)}(k) = \frac{8}{3}\left(h_\ell\left(\frac{4}{27}\right) + \frac{4}{27} h'_\ell\left(\frac{4}{27}\right)\right) = \frac{6\ell(\ell+3)(2\ell+3)(\ell^2+3\ell+4)}{5(\ell+1)^2(\ell+2)^2} \overset{\ell\gg 1}{\sim} \frac{12}{5}\ell \tag{4.9}$$

which gives the average number of edges at distance ℓ from the root edge and *lying in the same baby universe* as this root edge. Indeed keeping k finite precisely amounts to conditioning the counted edge to lie in the same baby universe as the root edge. The above quantity may in this sense be viewed as the *two-point function inside a minbu*, which grows like ℓ at large ℓ instead of ℓ^3 for the local limit of the complete two-point function. Note that, even though the total size n is fixed, the size of the considered minbu (that containing the root edge) is here a fluctuating quantity so that our two-point function inside a minbu corresponds in practice to a grand-canonical ensemble of minbus (technically this explains why it involves the regular part of h_ℓ rather than its singular part).

Returning to the ensemble of quadrangulations with two marked edges at distance ℓ and conditioning again the size n, we may also consider the probability $w_\ell^{(n)}(m)$ that the two marked edges at distance ℓ be separated by exactly m minimal necks. This probability is computed in the appendix in the limit $n \to \infty$. It takes the simple form

$$w_\ell^{(\infty)}(m) \to \tfrac{16}{81}(m+1)\left(\tfrac{5}{9}\right)^m \qquad \text{for} \qquad \ell \to \infty. \tag{4.10}$$

Note that $\sum_{m\geqslant 0} \frac{16}{81}(m+1)\left(\frac{5}{9}\right)^m = 1$, which means that, even if the two marked edges are far apart, there is still a finite number of minimal necks to go through to reach one from the other. Now for $\ell \to \infty$, the two marked edges lie with probability 1 into two different baby universes and we moreover expect that a geodesic path between them goes through, say m_1 minimal necks in the vicinity (i.e. at a distance which remains finite when $\ell \to \infty$) of the first edge, then travels a distance of order ℓ in the mother universe, and finally goes through m_2 minimal necks in the vicinity of the second edge. The distribution of minimal necks in the vicinity of one of the two edges is a local property which does not depend on the second edge (provided it is far enough) and simply describes how the first edge is linked to the mother universe. The law $\wp(m_1)$ for m_1 and that for m_2 are the same by symmetry, and we have

$$\frac{16}{81}(m+1)\left(\frac{5}{9}\right)^m = \sum_{m_1+m_2=m} \wp(m_1)\wp(m_2) \tag{4.11}$$

from which we deduce the law for the number m_1 of minimal necks to go through to reach the mother universe from the first edge:

$$\wp(m_1) = \tfrac{4}{9}\left(\tfrac{5}{9}\right)^{m_1}. \tag{4.12}$$

In particular, we have a probability $\wp(0) = 4/9$ that the first component of the kernel, i.e. that closest to the first edge, be the mother universe itself. Note that this probability is slightly greater than the known probability $1/3$ that the marked edge belongs to the mother universe. This is because, with our definition of kernel, it is sufficient for having $m_1 = 0$ that the first edge has the same extremities as an edge belonging to the mother universe. Note that the law $\wp(m_1)$ is in practice a property of simply rooted quadrangulations and that the introduction of the second edge at distance ℓ was only instrumental in the calculation.

In the same spirit, we may more precisely study the law for the *distance from the origin of the root edge to the mother universe* in large rooted quadrangulations. The detailed calculation is presentated in the appendix. When $n \to \infty$, we find a probability

$$\pi(D) = \frac{4(5+2D)}{(D+2)^2(D+3)^2} \tag{4.13}$$

that the root edge be at a distance D from the mother universe.

5. Discussion and conclusion

In this paper, we have presented a detailed calculation of the two-point function for quadrangulations with no multiple edges, based on a coding of these maps by well-balanced well-labeled trees. These trees could be enumerated exactly, for instance via a simple substitution procedure relating the known generating functions (Q_ℓ, F_ℓ and H_ℓ) for regular well-labeled trees to generating functions (q_ℓ, f_ℓ and h_ℓ) for almost well-balanced trees and by then extracting from these generating functions the contributions (p_ℓ, e_ℓ and g_ℓ) of fully well-balanced ones.

In the scaling limit, the two-point function of quadrangulations with no multiple edges of size n matches precisely that of general quadrangulations of size $3n$. This is consistent with the picture of a general quadrangulation of size $3n$ as made of a mother universe with no multiple edges of size n with attached baby universes of size negligible with respect to n. In large general quadrangulations, two generic points at a large mutual distance will lie in different baby universes so that the geodesics between them will travel mostly within the mother universe. More precisely, the probability that two marked points at distance ℓ lie in the same baby universe tends to zero like $1/\ell^2$ and by taking $\ell \to \infty$, we may therefore guarantee that any path linking them enters the mother universe. We used this property to compute the law for the distance of a random point to the mother universe or for the number of necks to go through to reach this mother universe.

A different two-point function is obtained by conditioning the two marked points to lie in the same baby universe, which can be done by requiring that the associated kernel be finite. In this case, the geodesics between the two points do not enter the mother universe and this leads to a new two-point function *inside* a baby universe, which we computed in the local limit. At large distance ℓ, it grows as ℓ instead of ℓ^3.

Our results deal with minimal neck baby universes only, which, as apparent on the two-point function, disappear in the scaling limit of large maps. Still, a more general baby universe structure should remain visible in the scaling regime, involving larger necks of size of order $n^{1/4}$. This structure is revealed for instance by the phenomenon of confluence of geodesics, but no precise rigorous statement was made so far to corroborate this picture. In

this respect, it would of course be desirable to be able to eliminate cycles of arbitrary size in large quadrangulations. We however here face the problem of having a canonical prescription of which cycles to eliminate and which to retain in the mother universe. The case of cycles of length 4 in quadrangulations with no multiple edges is still tractable and removing non-contractible cycles of length 4 is known to correspond in the equivalence with general maps to going from 2-connected to 3-connected ones. Keeping track of distances while removing these cycles seems to be a tractable issue.

A much simpler question is that of more general maps, for instance $2p$-angulations ($p > 2$) with no multiple edges. We have indeed a well-labeled mobile description of these maps [23] in general and removing double edges again simply amounts to making these mobiles well-balanced. By a simple substitution procedure, we can obtain the generating function p_1 of rooted $2p$-angulations with no multiple edges with a weight z per face:

$$p_1 = z\binom{2p-1}{p} r^{p-1} - \binom{2p-1}{p+1} r^p$$
$$\text{with} \qquad r = 1 + z\binom{2p-1}{p+1} r^{p+1} \tag{5.1}$$

and there seems to be no technical problem to address the question of the distance-dependent two-point function in this case.

Finally, it seems also possible to address the question of the three-point function in quadrangulations with no multiple edges. Again we expect to recover at large distances that of general quadrangulations, up to a global rescaling of the size by a factor of 3.

Appendix

We consider here the ensemble of quadrangulations with two marked edges at distance ℓ and with size n. The probability $w_\ell^{(n)}(m)$ that the two marked edges be separated by exactly m minimal necks reads (for $\ell \geqslant 1$)

$$w_\ell^{(n)}(m) = \frac{R_1^2\left(\delta_{m,0} + \left[\hat{g}\left(t, gR_1^2\right)\right]^{m+1}\right)\big|_{t^{\ell-1}g^n}}{H_\ell|_{g^n}} = \frac{R_1^2\left(\delta_{m,0} + \left[1 - \frac{R_1^2}{\hat{H}(t,g)}\right]^{m+1}\right)\Big|_{t^{\ell-1}g^n}}{H_\ell|_{g^n}} \tag{A.1}$$

where we used $\hat{g}(t, z(g)) = 1 - 1/\hat{h}(t, z(g)) = 1 - R_1^2/\hat{H}(t, g)$ upon introducing

$$\hat{H}(t, g) \equiv \sum_{\ell \geqslant 0} H_{\ell+1}(g) t^\ell. \tag{A.2}$$

To extract the large n leading behavior of the g^n coefficients, we use the expansions

$$R_1^2 = \tfrac{16}{9}(1 - 2\epsilon^2 + 4\epsilon^3 + \cdots) \tag{A.3}$$

and

$$\hat{H}(t, g) = \hat{A}^{(H)}(t) + \hat{C}^{(H)}(t)\epsilon^2 + \hat{D}^{(H)}(t)\epsilon^3 + \cdots \tag{A.4}$$

with, in particular,

$$\hat{A}^{(H)}(t) = \frac{4(-3t^2 + 4\mathrm{Li}_2(t)t + 4t - 4\mathrm{Li}_2(t))}{t^3} \overset{t\to 1}{\to} 4$$
$$\hat{D}^{(H)}(t) = \sum_{\ell \geqslant 0} D_{\ell+1} t^\ell \overset{t\to 1}{\sim} \frac{96}{7(1-t)^4}. \tag{A.5}$$

Picking the leading singularity (coefficient $\propto \epsilon^3$) of both the numerator and the denominator of (A.1), we deduce that, for $n \to \infty$,

$$w_\ell^{(\infty)}(m) = \frac{\frac{16}{9}\left[1-\frac{16}{9\hat{A}^{(H)}(t)}\right]^m \left[4\left(1-\frac{16}{9\hat{A}^{(H)}(t)}+\delta_{m,0}\right)+\frac{16(m+1)}{9\hat{A}^{(H)}(t)}\left(\frac{\hat{D}^{(H)}(t)}{\hat{A}^{(H)}(t)}-4\right)\right]\Big|_{t^{\ell-1}}}{\hat{D}^{(H)}(t)|_{t^{\ell-1}}}$$

$$\overset{\ell\gg 1}{\sim} \left(\frac{16}{9\hat{A}^{(H)}(1)}\right)^2 (m+1)\left[1-\frac{16}{9\hat{A}^{(H)}(1)}\right]^m = \frac{16}{81}(m+1)\left(\frac{5}{9}\right)^m \tag{A.6}$$

since the large ℓ behavior is entirely dictated by the $t \to 1$ limit.

We may alternatively study the law for the *distance from the origin of root edge to the mother universe* in large rooted quadrangulations. It may be obtained by first computing the law for the distance to the first minimal neck to go through to reach the mother universe. We call this distance d if the first minimal neck is formed of two $d \to (d+1)$ edges. We have in particular $d = 0$ if the first neck consists of two $0 \to 1$ edges, with the extremity at distance 1 necessarily different from the extremity of the root edge. By convention, if the root edge already 'touches' the mother universe (i.e. belongs to the mother universe or has the same extremities as an edge belonging to the mother universe), we set $d = \infty$ as there is no first minimal neck in this case. The probability law for d may again be obtained by temporarily introducing a second marked edge at distance ℓ and then sending $\ell \to \infty$. It reads

$$\begin{aligned} P(d) &= \lim_{\ell\to\infty}\lim_{n\to\infty} \frac{R_1^2\, g_{d+1}\left(gR_1^2\right) h_{\ell-d}\left(gR_1^2\right)\big|_{g^n}}{H_\ell|_{g^n}} \\ &= \lim_{\ell\to\infty} \frac{\left(1-\frac{16}{9\hat{A}^{(H)}(t)}\right)\Big|_{t^d} \hat{D}^{(H)}(t)|_{t^{\ell-d-1}} + \left(\frac{16}{9\hat{A}^{(H)}(t)}\left(\frac{\hat{D}^{(H)}(t)}{\hat{A}^{(H)}(t)}-4\right)\right)\Big|_{t^d} \hat{A}^{(H)}(t)|_{t^{\ell-d-1}}}{\hat{D}^{(H)}(t)|_{t^{\ell-1}}} \\ &= \left(1-\frac{16}{9\hat{A}^{(H)}(t)}\right)\Big|_{t^d} \end{aligned} \tag{A.7}$$

or equivalently

$$\sum_{d\geqslant 0} P(d)t^d = 1-\frac{16}{9\hat{A}^{(H)}(t)} = \frac{1}{5}+\frac{7}{25}t+\frac{79}{2500}t^2+\frac{699}{50\,000}t^3+\frac{1910\,211}{245\,000\,000}t^4+\cdots \tag{A.8}$$

where we explicited the first values of $P(d)$ for $d = 0, 1, 2, 3, 4$. We have in particular a probability $\sum_{d\geqslant 0} P(d) = 5/9$ that we have to go through at least a minimal neck to reach the mother universe and, if so, the distance to this minimal neck is on average $\sum_{d\geqslant 0} d\,P(d)/\sum_{d\geqslant 0} P(d) = (4/5)(2\pi^2/3-5) = 1.263\,79\ldots$. The complementary probability $4/9$ is that of the event of a root edge touching the mother universe. This is consistent with the value $\wp(0) = 4/9$. For large d, we find from the singular behavior of $A^{(H)}(t)$ at $t = 1$ that $P(d)/\sum_{d\geqslant 0} P(d) \sim 32/(5d^3)$. Note that along the same lines, we can as well compute the joint probability for the distance d to the first minimal neck and for the size k of the component linking the root edge to this neck. We find a probability $g_{d+1}|_{z^k}(4/27)^k$, which, as it should adds up to $P(d)$ upon summing over k.

Consider now the total distance D from the origin of the root edge to the mother universe in large quadrangulations. This distance is 0 if the root edge touches the mother universe or if it is separated from the mother universe only by (nested) necks made of pairs of $0 \to 1$ edges only. The law for D may be deduced from $P(d)$ above upon writing

$$\pi(D) = \tfrac{4}{9}\delta_{D,0} + P(D)\tfrac{4}{9} + P * P(D)\tfrac{4}{9} + P * P * P(D)\tfrac{4}{9} + \cdots \tag{A.9}$$

where $P * Q(D) = \sum_{d=0}^{D} P(D)Q(d-D)$ is a simple convolution. Indeed, any geodesic path to the mother universe generically crosses a number m of necks and may accordingly be decomposed into m pieces whose lengths add up to D and share *the same probability law* P. This leads to a probability $P^{*m}(D)$, to be summed over m. We get finally

$$\sum_{D\geqslant 0} \pi(D)t^D = \frac{4}{9}\frac{1}{1-\sum_{D\geqslant 0} P(D)}t^D$$

$$= \frac{\hat{A}^{(H)}(t)}{4} = \sum_{D\geqslant 0} \frac{A_{D+1}}{4}t^D \tag{A.10}$$

with in particular $\sum_{D\geqslant 0}\pi(D) = 1$. We deduce

$$\pi(D) = \frac{A_{D+1}}{4} = \frac{4(5+2D)}{(D+2)^2(D+3)^2}. \tag{A.11}$$

In particular, the average distance is $2\pi^2/3 - 5 = 1.579\,74\ldots$ and for large D, we have $\pi(D) \sim 8/D^3$.

References

[1] Kazakov V 1985 Bilocal regularization of models of random surfaces *Phys. Lett.* B **150** 282–4
David F 1985 Planar diagrams, two-dimensional lattice gravity and surface models *Nucl. Phys.* B **257** 45–58
Ambjørn J, Durhuus B and Fröhlich J 1985 Diseases of triangulated random surface models and possible cures *Nucl. Phys.* B **257** 433–49
Kazakov V, Kostov I and Migdal A 1985 Critical properties of randomly triangulated planar random surfaces *Phys. Lett.* B **157** 295–300

[2] for a review, see Di Francesco P, Ginsparg P and Zinn-Justin J 1995 2D gravity and random matrices *Phys. Rep.* **254** 1–131

[3] Marckert J F and Mokkadem A 2006 Limit of normalized quadrangulations: the Brownian map *Ann. Probab.* **34** 2144–202 (arXiv:math.PR/0403398)

[4] Le Gall J F 2007 The topological structure of scaling limits of large planar maps *Invent. Math.* **169** 621–70 (arXiv:math.PR/0607567)

[5] Le Gall J F and Paulin F 2008 Scaling limits of bipartite planar maps are homeomorphic to the 2-sphere *Geomet. Funct. Anal.* **18** 893–918 (arXiv:math.PR/0612315)

[6] Miermont G 2008 On the sphericity of scaling limits of random planar quadrangulations *Electron. Commun. Probab.* **13** 248–57 (arXiv:0712.3687 [math.PR])

[7] Le Gall J-F 2010 Geodesics in large planar maps and in the Brownian map *Acta Math.* at press (arXiv:0804.3012 [math.PR])

[8] Bouttier J and Guitter E 2008 The three-point function of planar quadrangulations *J. Stat. Mech.* P07020 (arXiv:0805.2355 [math-ph])

[9] Bouttier J and Guitter E 2009 Confluence of geodesic paths and separating loops in large planar quadrangulations *J. Stat. Mech.* P03001

[10] Ambjørn J, Durhuus B and Jonsson T 1997 *Quantum Geometry: A Statistical Field Theory Approach* (Cambridge: Cambridge University Press)

[11] Ambjørn J and Watabiki Y 1995 Scaling in quantum gravity *Nucl. Phys.* B **445** 129–44 (arXiv:hep-th/9501049)

[12] Ambjørn J, Jurkiewicz J and Watabiki Y 1995 On the fractal structure of two-dimensional quantum gravity *Nucl. Phys.* B **454** 313–42 (arXiv:hep-lat/9507014)

[13] Bouttier J, Di Francesco P and Guitter E 2003 Geodesic distance in planar graphs *Nucl. Phys.* B **663** 535–67 (arXiv:cond-mat/0303272)

[14] Gao Z and Wormald N C 1999 The size of the largest components in random planar maps *SIAM J. Discrete Math.* **12** 217–28

[15] Banderier C, Flajolet P, Schaeffer G and Soria M 2001 Random maps, coalescing saddles, singularity analysis, and airy phenomena *Random Struct. Algorithms* **19** 194–246

[16] Jain S and Mathur S 1992 World-sheet geometry and baby universes in 2D quantum gravity *Phys. Lett.* B **286** 239–46 (arXiv:hep-th/9204017)

[17] Marcus M and Schaeffer G 2001 Une bijection simple pour les cartes orientables, available at http://www.lix.polytechnique.fr/Labo/Gilles.Schaeffer/Biblio/
Schaeffer G 1998 Conjugaison d'arbres et cartes combinatoires aléatoires *PhD Thesis* Université Bordeaux I
Chapuy G, Marcus M and Schaeffer G 2009 A bijection for rooted maps on orientable surfaces *SIAM J. Discrete Math.* **23** 1587–611 (arXiv:0712.3649 [math.CO])
[18] Chapuy G and Schaeffer G 2009 private communication
[19] Tutte W T 1963 A census of planar maps *Can. J. Math.* **15** 249–71
[20] Brown W G 1963 Enumeration of nonseparable planar maps *Can. J. Math.* **15** 526–54
[21] Brown W G and Tutte W T 1964 On the enumeration of rooted nonseparable planar maps *Can. J. Math.* **16** 572–7
[22] Schaeffer G and Jacquard B 1998 A bijective census of nonseparable planar maps *J. Comb. Theory* A **83** 1–20
[23] Bouttier J, Di Francesco P and Guitter E 2004 Planar maps as labeled mobiles *Electron. J. Comb.* **11** R69 (arXiv:math.CO/0405099)